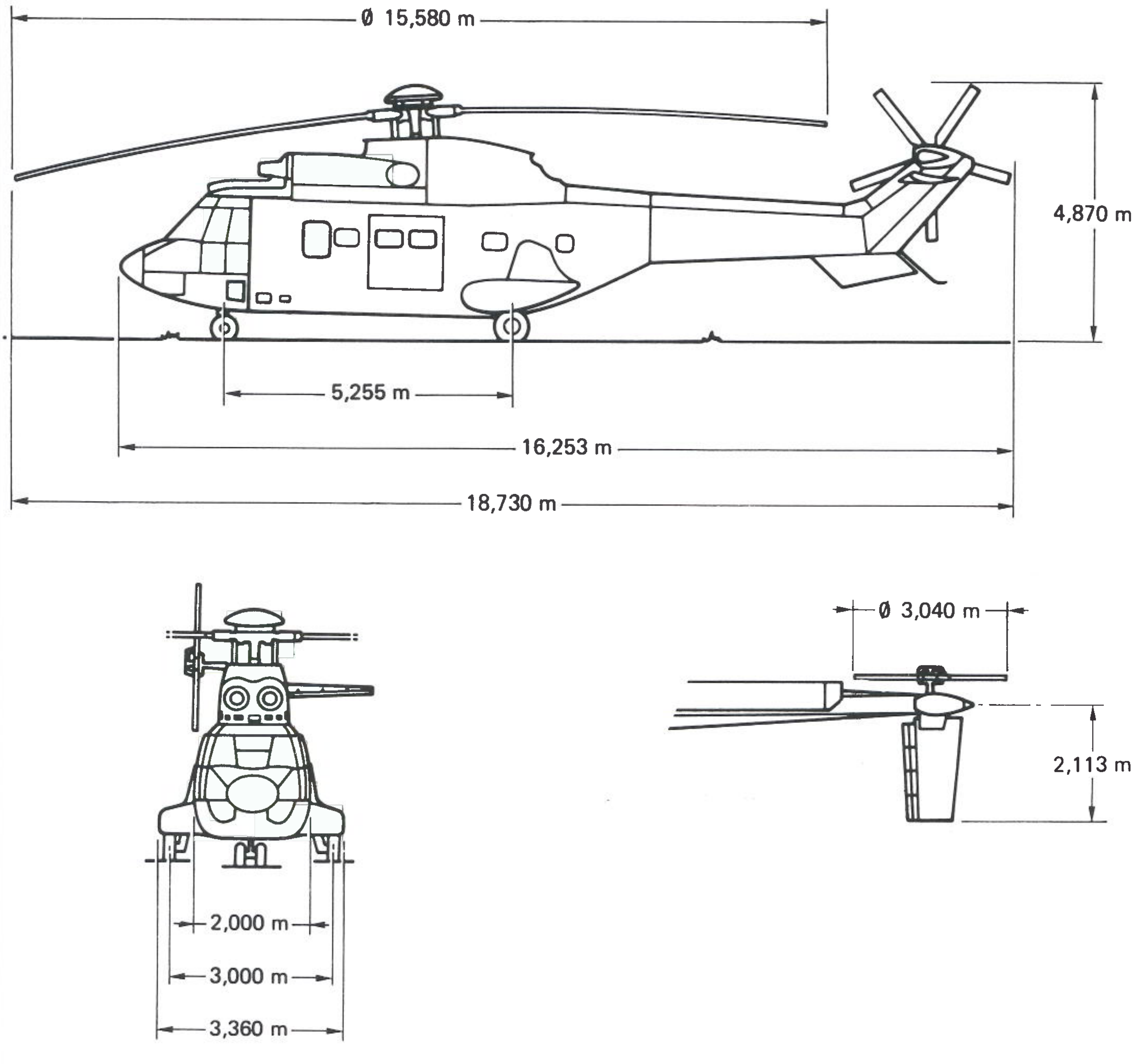

Figure 1: Showing general layout of AS332L.

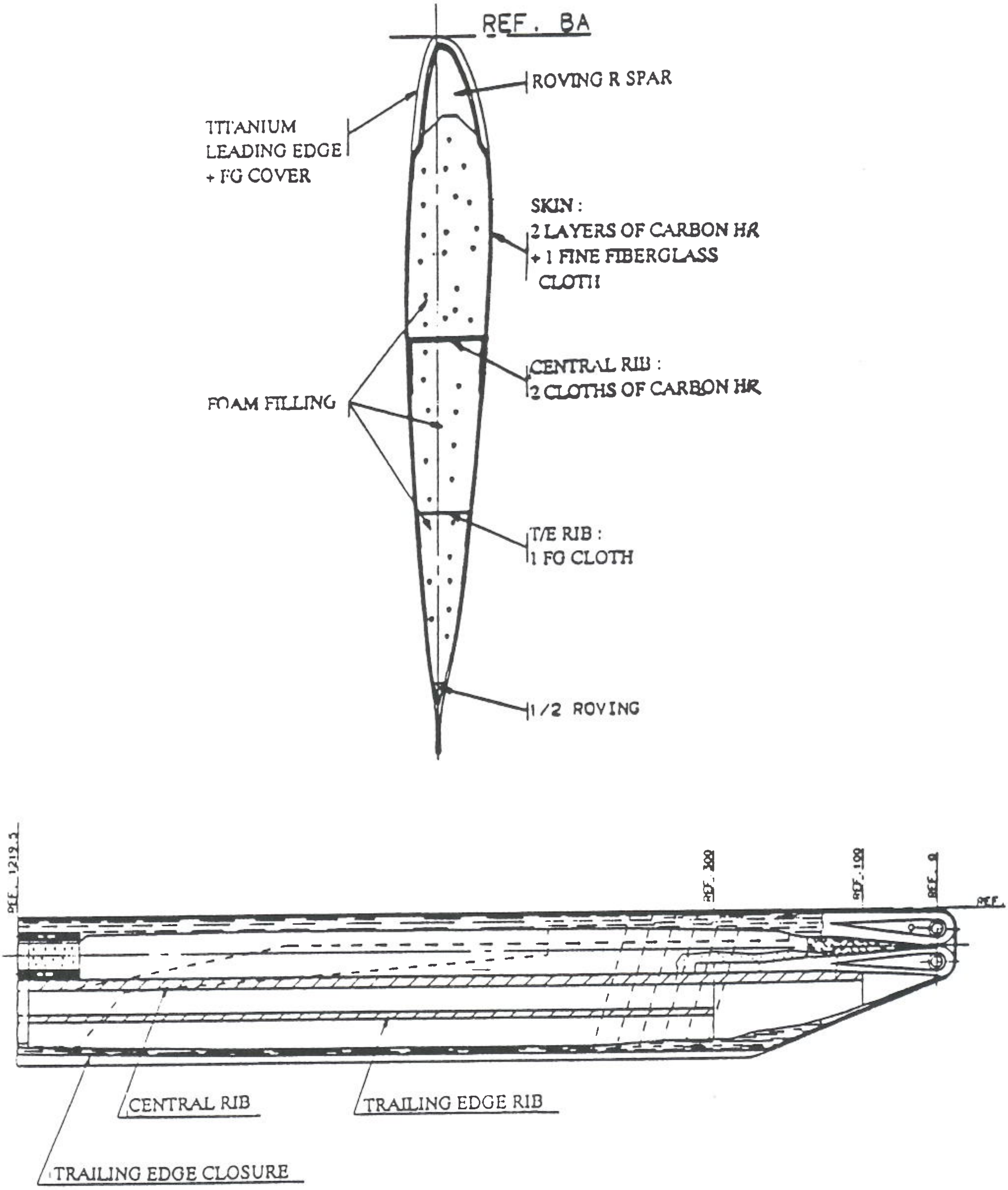

Figure 2: Showing tail rotor blade structure.

Figure 3: Showing a sample tail rotor blade with leading edge anti-erosion shield, plastic cover overlying brass strip and braided bonding strap to root bolt.

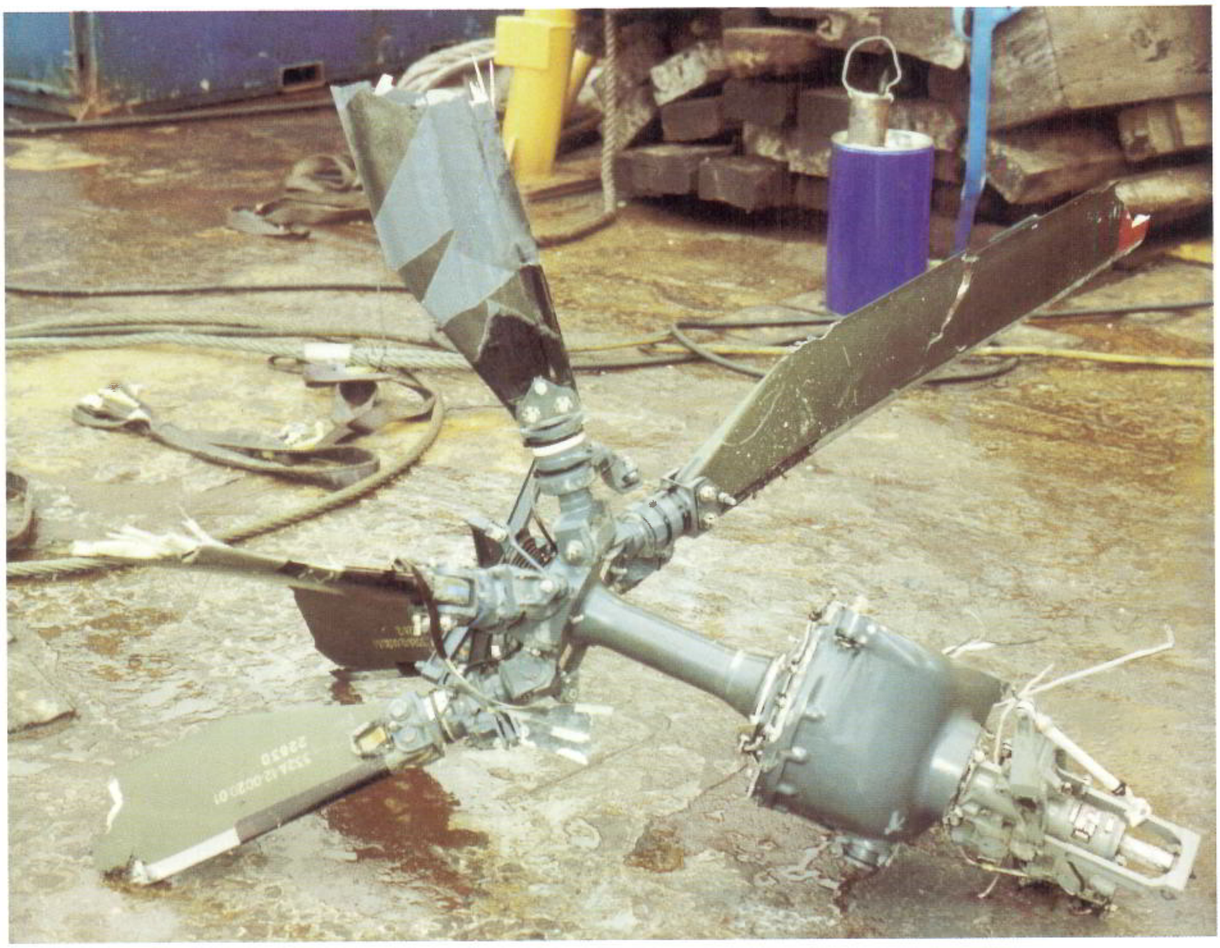

Figure 4A: Showing recovered tail rotor, gearbox and pitch servo assembly, with 'White' blade root section uppermost.

Figure 4B: Showing outboard side of 'White' tail rotor blade root with leading edge erosion shield and brass strip missing, and failed braided bonding strap.

Figure 5: Showing deep gash in trailing edge of tail boom pylon and tail rotor blade impact damage on right side.

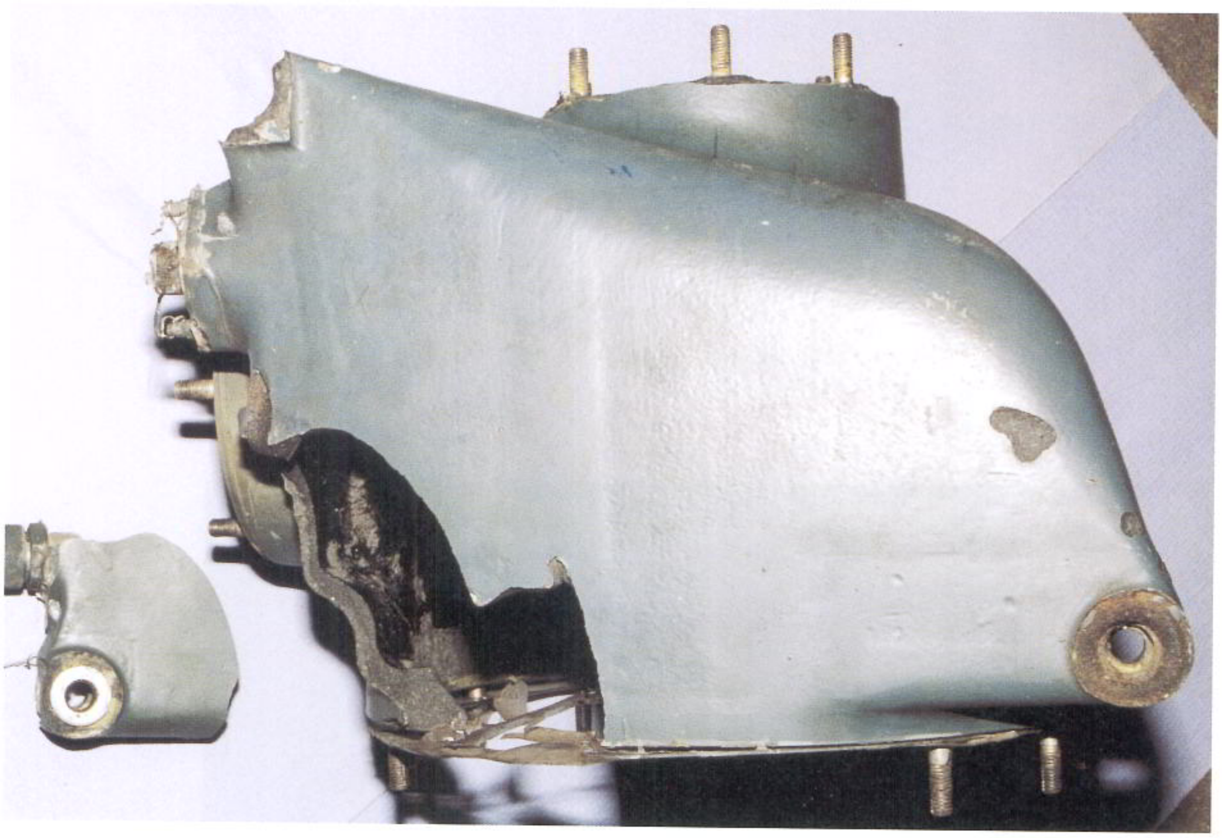

Figure 6: Showing failed lower attachments of gearbox (left attachment is upper one in this photograph, right is lower).

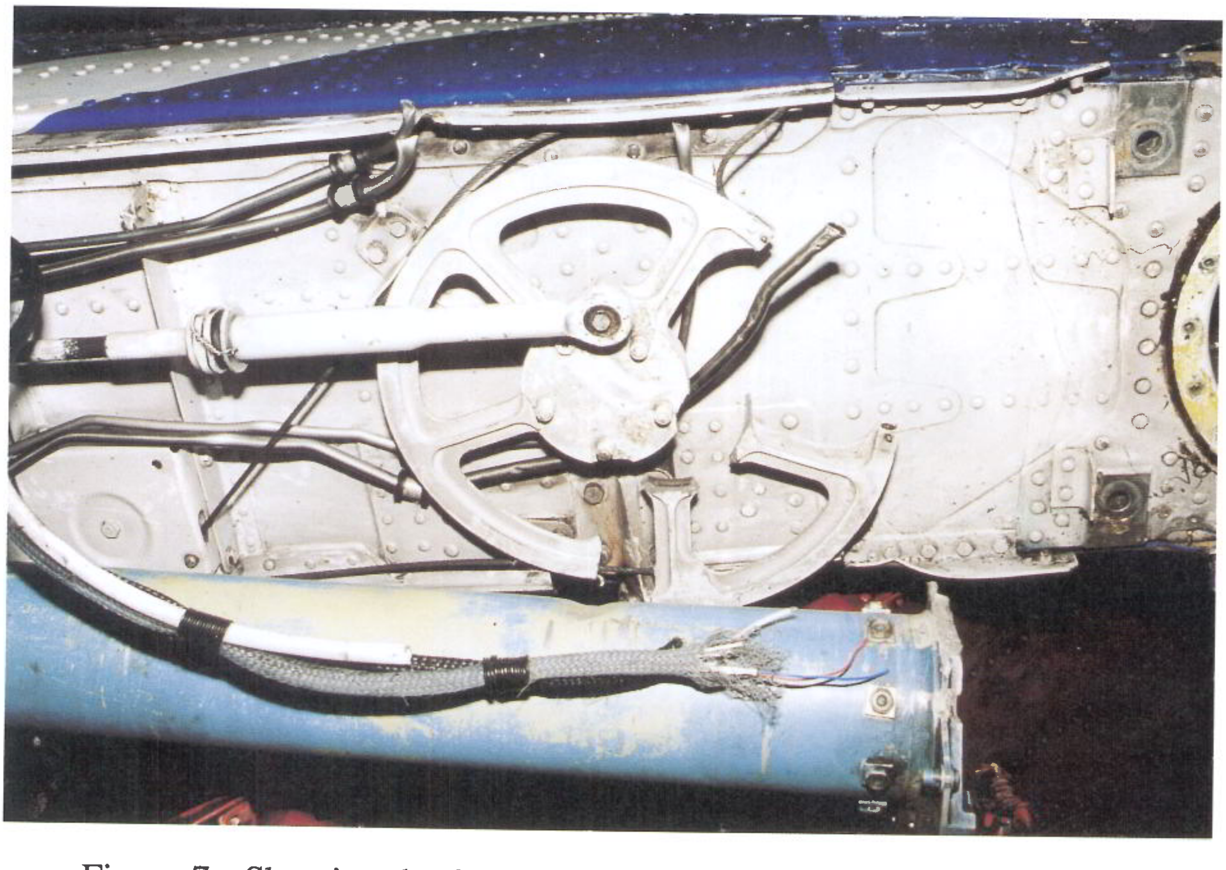

Figure 7: Showing the four severed hydraulic pipes, with two right side pipes sharply bent around damaged right support flange.

Figure 8: Showing recovered inboard section of 'Blue' main rotor blade with bonding strip missing, alongside 'Yellow' MRB for comparison.

Figure 9A: Showing localised blade skin damage at overlap of leading edge anti-erosion shield sections due to related arcing on 'Black' MRB.

Figure 9B: Showing all recovered main rotor blade sections, with 'Blue' blade in foreground and 'Black' blade sections in background.

Figure 10: Showing damaged outboard (right) side of 'White' tail rotor blade, with thermal delamination of root area, full length fissure of composite within bonding strip recess and removal of leading edge skin layer under deatched anti-erosion shield.

Figure 11: Showing damaged inboard (left) side of 'White' tail rotor blade, with thermal delamination of root area and general delamination outboard, including the leading edge from which the anti-erosion shield detached.

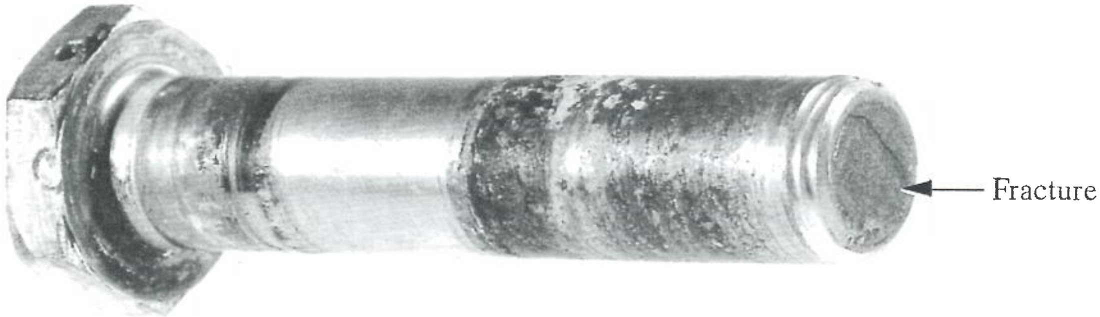

Figure 12A: Showing upper length of tail rotor gearbox upper attachment bolt with fracture face arrowed.

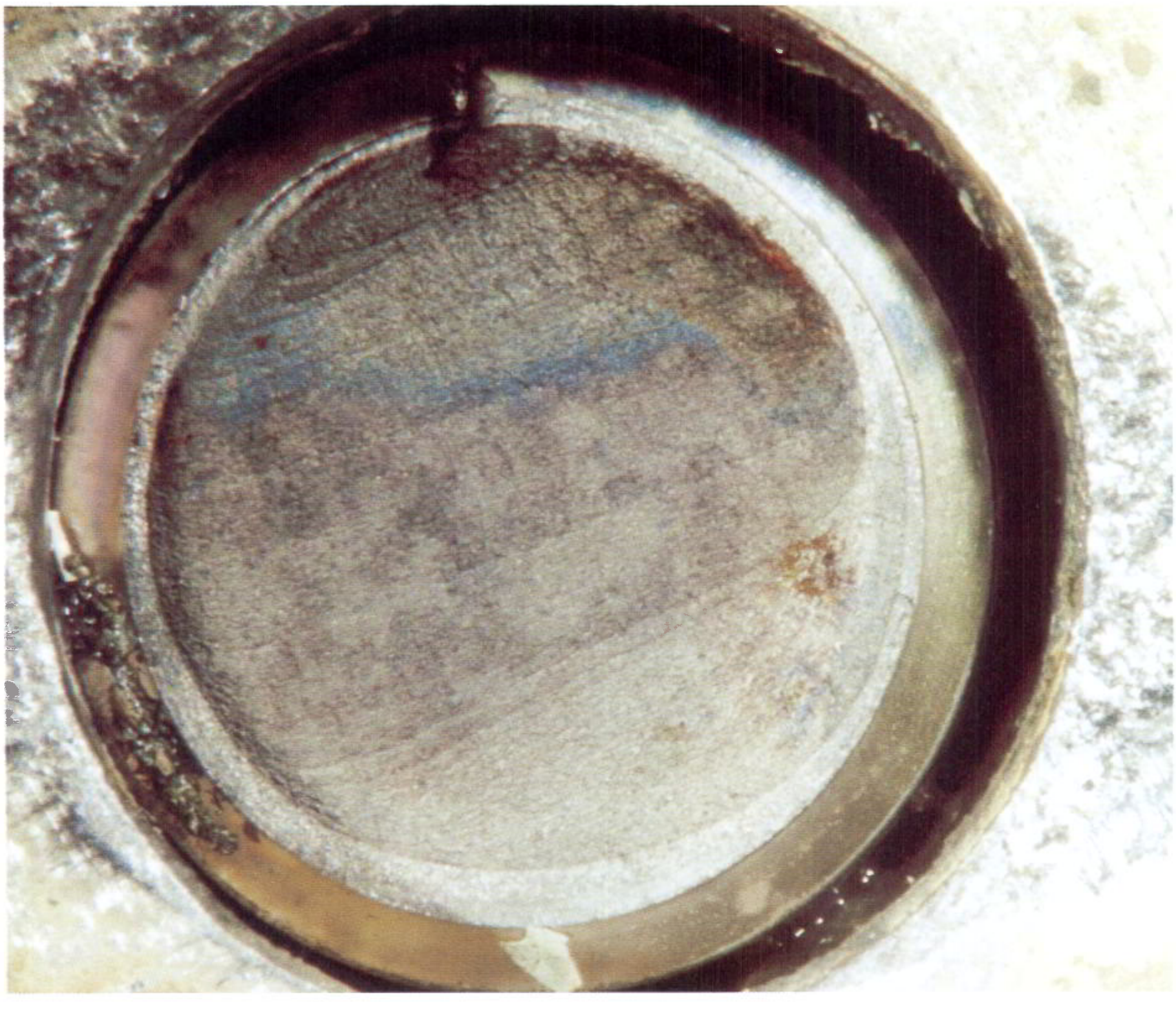

Figure 12B: Showing fracture surface of lower (threaded) end of tail rotor gearbox upper attachment bolt, with shallow (bright) annular band of initial radial fatigue propagation from the thread root, and secondary bending fatigue striations clearly evident emanating from upper arc, before the final overload failure evident within lower segment of fracture.

Figure 13: Showing the recovered tail rotor blade sections with, left to right in this photograph, 'White', 'Red', 'Blue' and 'Black' blades, outboard (right) sides uppermost. Note similar lengths of first four severed blades, caused by rotational penetration into aft side of pylon (Figure 5, A-6).

Figure 14: Showing the recovered helicopter onboard MSV Stadive without its main rotor head and main gearbox assembly which detached during the first associated 'lift' from the seabed and was recovered before the main airframe structure shown here.

APPENDIX B

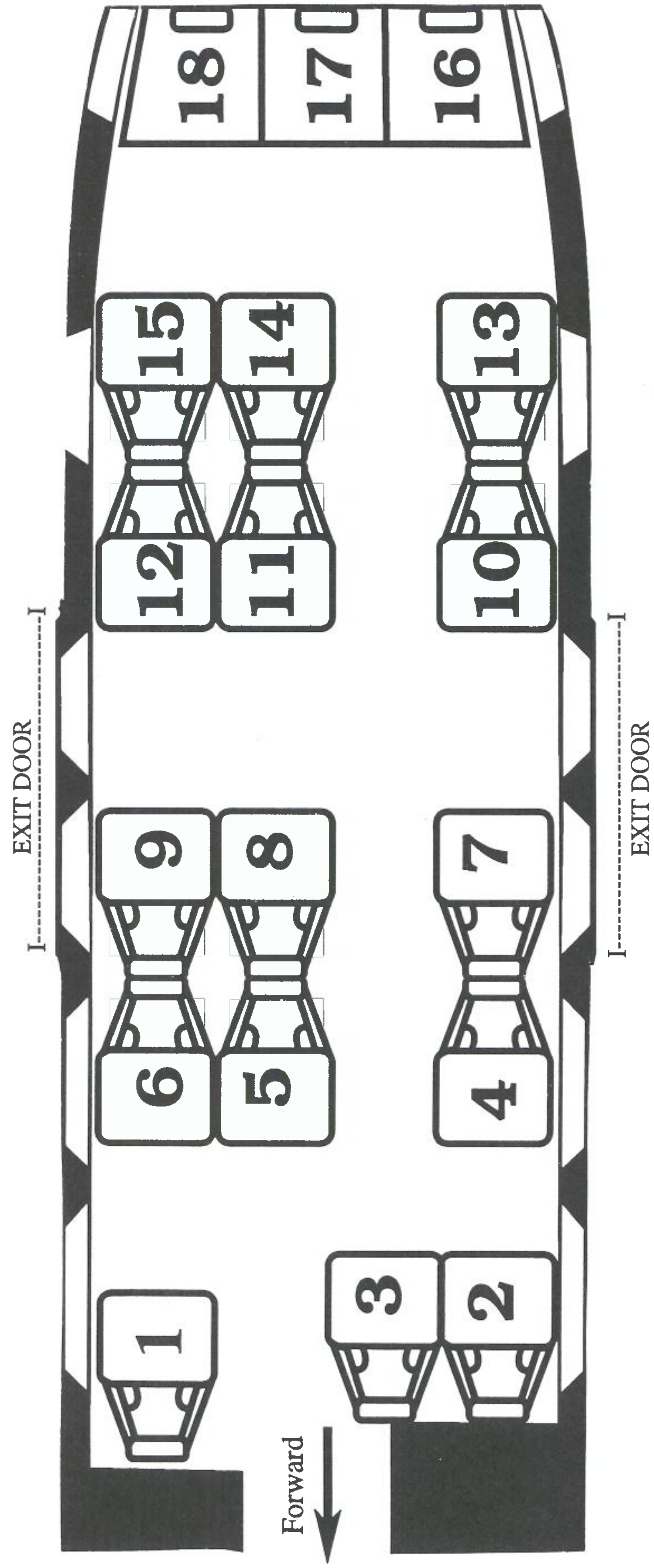

Figure 1: Showing cabin seating layout.

Figure 2: Showing right main door emergency exit with both spring-loaded arms arrowed.

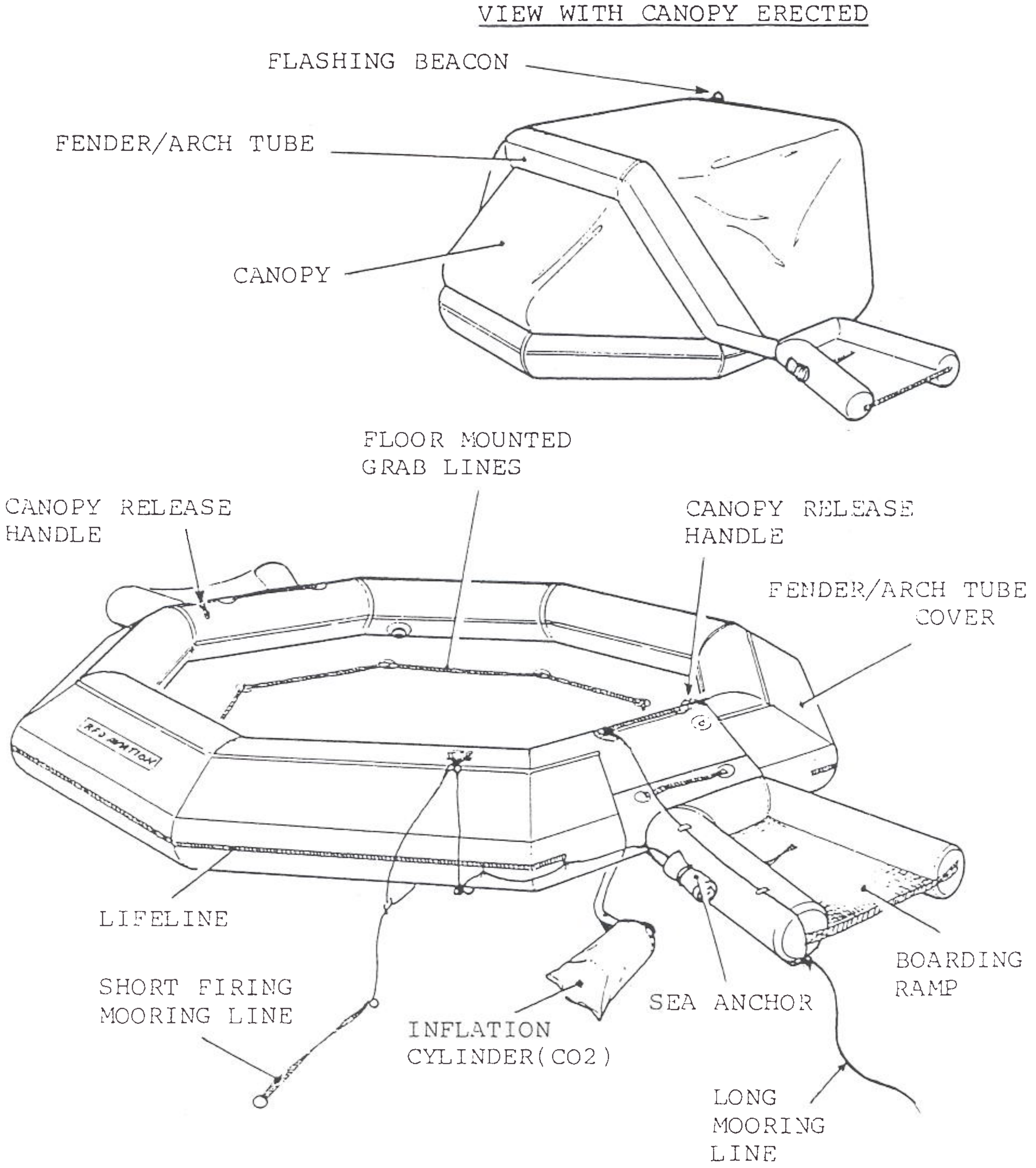

Figure 3: Showing general design features of the RFD Type 14R MK1 Liferaft.

Figure 4: Showing location of the automatically deployable emergency locator transmitter (ADELT) housing.

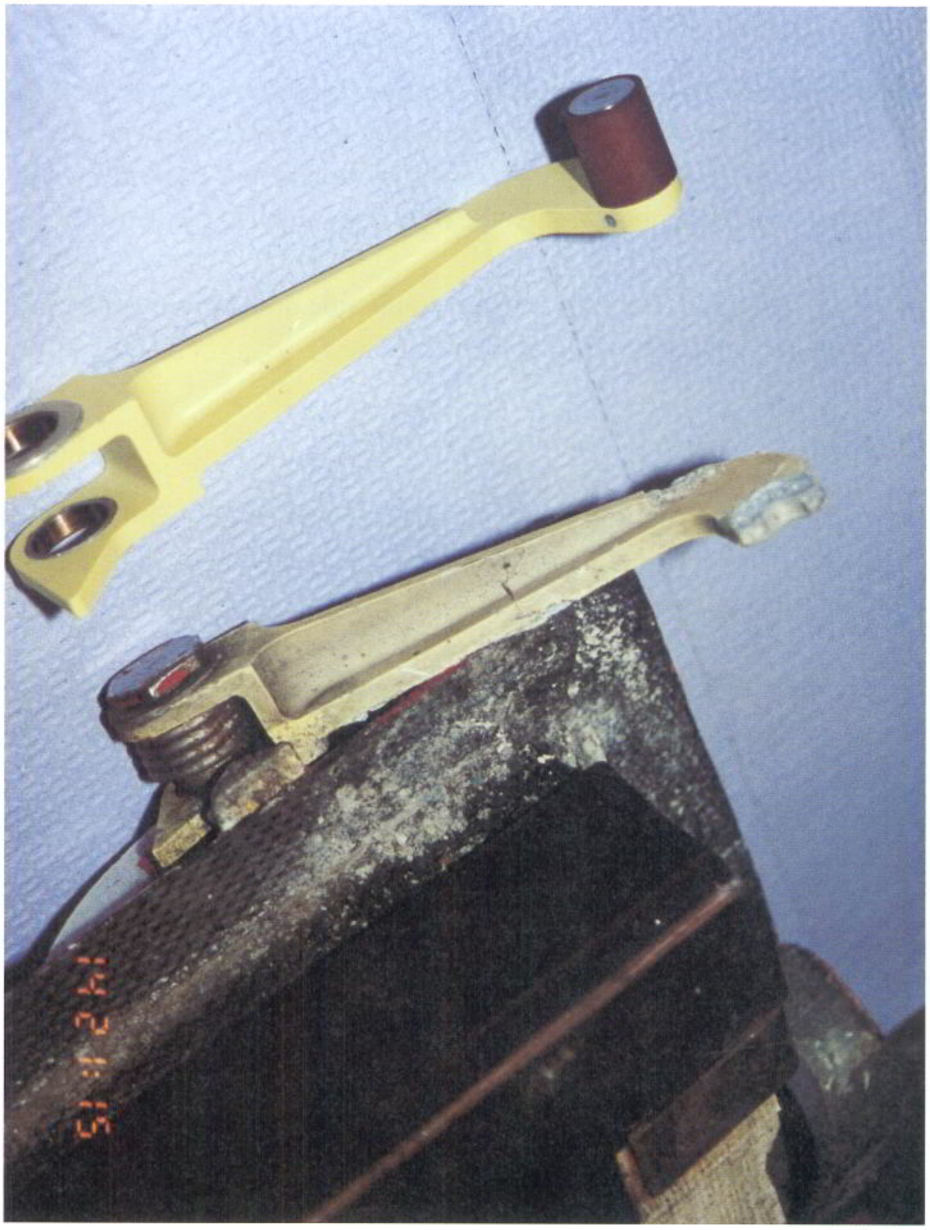

Figure 5: Showing hook-shaped broken end of spring-loaded arm at upper forward corner of left main door, after detachment of roller end, with new arm/roller for comparison; aft arm on this door and forward arm on right door were also broken in this manner.

THE EVACUATION

Interviews with the occupants of the helicopter revealed the following information regarding their initial actions and their means of evacuation from G-TIGK:

Cockpit:

Commander (right seat): After the ditching, he applied the rotor brake, released his side door, operated the jettison handle for the right hand cabin door and then switched off all non-essential systems before moving back to the cabin, picking up a survival pack from the back of the cockpit/cabin bulkhead and evacuating through the right door and into the heliraft.

First officer (left seat): After the ditching, he released his side door before going back to the cabin and evacuating through the right door and into the heliraft.

Cabin:

Seat No. 1: After the second bang, the occupant released part of the window beading from the front right window; after the ditching, he knocked the front right window out and was the second man out of that window and into the heliraft.

Seat No. 2: The occupant knocked out the front left window after the ditching and then was the fifth man out of that window and into the heliraft.

Seat No. 3: After the ditching, the occupant was the fourth man out of the front right window and into the heliraft.

Seat No. 4: After the ditching, the occupant had started to release the second left window, but then went back towards the left door; as the left door aperture had the inflated heliraft blowing against it, he went to the right door and evacuated into the heliraft.

Seat No. 5: After the ditching, the occupant pulled the right door emergency release mechanism, and then was the third man out of the front right window.

Seat No. 6: After the ditching, the occupant began to pull the beading from the second right window, but then assisted in releasing the front right window and was the first man out of that window and first into the heliraft.

Seat No. 7: Initially this seat was unoccupied but after the first bang the occupant of Seat 8 moved to this position; just before the ditching, he removed the beading from both windows of the left door and then knocked them both out as the helicopter alighted. After the rotors stopped, he assisted in pushing the left door out, pulled the heliraft from under Seat 10, connected the painter and threw the heliraft out of the left door. It inflated, but kept blowing against the open door. He then went to the right door and boarded the heliraft.

Seat No. 8: The occupant moved to Seat 7 following the initial bang.

Seat No. 9: As the helicopter was descending the occupant retained a grip on the beading of the front window of the right door and, on ditching, released the window and assisted in kicking the right door out. He assisted in inflating the right heliraft and was first out of the right door, and second into the heliraft.

Seat No. 10: After the ditching, the occupant assisted in opening the left door and inflating the heliraft. With some problems apparent in launching the left heliraft, he went to the right door and boarded the heliraft.

Seat No. 11: After the ditching, the occupant assisted in pushing the right door out and was fourth, or fifth, out of that door and into the heliraft.

Seat No. 12: As the helicopter alighted, the occupant was removing the beading from the rear right door window. He then assisted in pushing out the right door and inflated the heliraft; he was second through the right door and into the heliraft.

Seat No. 13: After the ditching, the occupant was the sixth man through the right door and into the heliraft.

Seat No. 14: After the ditching, the occupant evacuated through the right door and into the heliraft.

Seat No. 15: After the ditching, the occupant started pulling the beading from the second rear window, but then evacuated through the right door and was the fifteenth man into the heliraft.

Seat No. 16: After the first bang, the occupant removed the beading from the rear right window; after the second bang he pushed the window out. Following the ditching, he evacuated through the right door into the heliraft.

Seat No. 17: Unoccupied.

Seat No. 18: After the ditching, the occupant evacuated through the right door and into the heliraft.

EXAMINATION OF THE HELIRAFT BY RFD

Punctured buoyancy chamber: There was a large tear in the buoyancy chamber directly below the boarding ramp position (not in the fender as initially thought). The tear extended across the complete panel and some of the survivors heard air escaping from this area after boarding the heliraft. There was evidence of a puncture initiation point approximately at the centre of the panel, from where the tear propagated outward. The length of the cut was indicative of a large object forcing itself into the chamber, thus elongating the tear.

Detached floor lifeline: The lifeline is designed to enable survivors to stabilise themselves in rough conditions, but it is attached to the floor by a patch in a way such that, if sufficient force is applied to the line, the patch is pulled off the floor, rather than ripping the floor itself. In this case, the heliraft was swamped and carrying an overload of passengers and the force which had been applied to the patch was sufficient to detach it. If this had not been a design feature, the floor would have been damaged or torn, with serious consequences for the occupants.

Canopy erection: Having boarded the heliraft, normal procedure is to cut the appropriate two bridle loops, freeing the sea anchor to drop into the water and releasing the short blue firing and mooring line from the helicopter. This frees the heliraft and permits the canopy to be raised. In this instance, only the bridle for the short blue firing line was cut, which released the heliraft to float away from the helicopter. Although the sea anchor bridle was not cut, this did not prevent the anchor from being deployed, but it did inhibit it from dropping into the water and streaming effectively. It also prevented one side of the canopy from being raised because the roof support tube was partially restrained by the bridle.

Paddles and bailer: The survivors were able to locate the equipment bag containing the First Aid kit etc, which was stored in one of the two bags, but had difficulty in finding the paddles or the bailer. Because of the considerable number of agencies through which the heliraft had passed, before being available for examination, it was not possible to identify the reason for this.

The inflation cylinder: One of the survivors was hit on the head by the heliraft inflation cylinder. The cylinder was attached by a hose and umbilical cord to the inflation valves, causing it to hang in the water after deployment. This design is the most suitable system for reversible life rafts as attaching it to the floor on one side reduces the occupancy rating on that side. Depending on which way up the heliraft is inflated the distance from the waterline to the cylinder varies because it must travel over the fender and into the water. This results in the cylinder being closer to the surface of the water in one orientation than in the other. This could have resulted in the cylinder being lifted from the water by wave action and causing the reported injury.

APPENDIX B

(ENCLOSURE 3)

MEMORANDUM OF UNDERSTANDING ON THE CO-ORDINATION OF SEARCH AND RESCUE MARITIME INCIDENTS ARISING FROM AVIATION ACCIDENTS BETWEEN THE COASTGUARD AGENCY, THE DEPARTMENT OF TRANSPORT (CIVIL AVIATION DIVISION) AND THE MINISTRY OF DEFENCE

Whereas in the United Kingdom the Department of Transport ("DOT") is the authority responsible for civil maritime and civil aviation search and rescue ("SAR");

and whereas the Ministry of Defence ("MOD"), through the Aeronautical Rescue Co-ordination Centres (ARCC), is responsible, on behalf of the DOT, for the initiation and co-ordination of civil aviation SAR within the United Kingdom SAR Region ("UKSRR");

and whereas the Coastguard Agency, through Maritime Rescue Co-ordination Centres (MRCC), and sub-centres (MRSC) is responsible, on behalf of the DOT, for the initiation and co-ordination of civil maritime SAR in the UKSRR;

The Coastguard Agency, The Department of Transport and the Ministry of Defence desiring to draw up arrangements to ensure clear co-ordination of SAR maritime incidents arising from aviation accidents have reached the following understanding:

1. Control of SAR maritime incidents arising from aviation accidents shall rest with the rescue authority (whether ARCC or MRCC) that initiates the response, until it decides that the other is better placed to continue the response.

2. The initiating authority must immediately inform the other rescue authority of the incident. Consultation between the rescue authorities must also take place when the appointment of an on-scene co-ordinator is contemplated, including a review of which centre should most appropriately control the incident.

3. In an incident involving a military aircraft, control of the incident would always rest with the ARCC even if the Coastguard were first to learn of its ditching.

Signed at London on 3 March 1997

For the Department of Transport

For the Coastguard Agency

For the Ministry of Defence

EXTRACTS FROM AC20-53A
(pages 6-10 and Appendices 1-3)

10. LIGHTNING ATTACHMENT PHENOMENA.

a. Swept-Stroke Phenomenon.

(1) The lightning channel is somewhat stationary in air while it is transferring electrical charge. When an airplane is involved, the airplane becomes part of the channel. However, due to the speed of the airplane and the length of time that the lightning channel exists, the airplane can move relative to the lightning channel. When a forward extremity, such as a nose or wing mounted engine pod is an initial attachment point, the movement of the airplane through the lightning channel causes the channel to sweep back over the surface as illustrated in figure 1 of appendix 2, producing subsequent attachment points. This is known as the swept-stroke phenomenon. As the sweeping action occurs, the characteristics of the surface can cause the lightning channel to reattach and dwell at various surface locations for different periods of time, resulting in a series of discrete attachment points along the sweeping path.

(2) The amount of damage produced at any point on the airplane by a swept-stroke depends upon the type of material, the dwell time at that point, and the lightning currents which flow during the attachment. Both high peak current restrikes with intermediate current components and continuing currents may be experienced. Restrikes typically produce reattachment of the arc at a new point.

(3) When the lightning channel has been swept back to one of the trailing edges, it may remain attached at the point for the remaining duration of the lightning event. An initial attachment point at a trailing edge, of course, would not be subjected to any swept-stroke action, and therefore, this attachment point will be subjected to all components of the lightning event.

(4) The significance of the swept-stroke phenomenon is that portions of the vehicle that would not be targets for the initial attachment points of a lightning flash may also be involved in the lightning strike process as the lightning channel is swept backwards, although the channel may not remain attached at any single point for very long. On the other hand, strikes that reach trailing edges must be expected to remain attached there (hang-on) for the balance of their natural duration.

b. Lightning Strike Zone Definitions. To account for each of the possibilities described in the foregoing paragraphs, the following zones have been defined:

(1) Zone 1.

i. Zone 1A: Initial attachment point with low possibility of lightning arc channel hang-on.

ii. Zone 1B: Initial attachment point with high possibility of lightning arc channel hang-on.

(2) Zone 2.

i. Zone 2A: A swept-stroke zone with low possibility of lightning arc channel hang-on.

ii. Zone 2B: A swept-stroke zone with high possibility of lightning arc channel hang-on.

(3) Zone 3. All of the vehicle areas other than those covered by Zone 1 and 2 regions. In Zone 3, there is a low possibility of any attachment of the lightning channel. Zone 3 areas may carry substantial amounts of electrical current, but only by conduction between some pair of attachment points.

(4) The zone definitions are in basic agreement with the definitions of earlier versions of this Advisory Circular, except that the former Zones 1 and 2 have been subdivided to account for low and high possibilities of the lightning arc channel hang-on (figures 2 & 3) shown in appendix 2. The locations of these zones on any airplane are dependent on the airplane's geometry and operational factors, and often vary from one airplane to another.

c. Location of Lightning Strike Zones. With these definitions in mind, the locations of each zone on a particular airplane may be determined as follows:

(1) Extremities such as the nose, wing and empennage tips, tail cone, wing-mounted nacelles, and other significant projections should be considered as within a direct strike zone because they are probable initial leader attachment points. Those that are forward extremities or leading edges should be in Zone 1A, and extremities that are trailing edges should be in Zone 1B. Most of the time, the first return stroke will arrive shortly after the leader has attached to the airplane, so Zone 1A is limited to the immediate vicinity (i.e., approximately 18 inches (0.5m) aft) of the forward extremity. However, in rare cases the return stroke may arrive somewhat later, thereby exposing surfaces further aft to this environment. This possibility should be considered if the probability of a flight safety hazard due to a Zone 1A strike to an unprotected surface is high.

(2) Where questions arise regarding the identification of initial attachment locations or where the airframe geometry is unlike conventional designs for which previous experience is available, scale model attachment point tests may be in order. Information on model testing can be found in the User's Manual.

(3) Surfaces directly aft of Zone 1A should be considered as within Zone 2A. Generally, Zone 2A will extend the full length of the surface aft of Zone 1A, such as the fuselage, nacelles, and portions of the wing surfaces.

(4) Trailing edges of surfaces aft of Zone 2A should be considered Zone 2B, or Zone 1B if initial attachment to them can occur. If the trailing edge of a surface is totally non-conductive, then Zone 2B (or 1B) should be projected forward and/or inboard to the nearest conductive surface.

(5) Surfaces approximately 18 inches (0.5m) to either side of initial- or swept-attachment points established by steps (1) and (2) of paragraph c should also be considered as within the same zone, to account for small lateral movements of the sweeping channel and local scatter among attachment points. For example, the tip of a wing would normally be within Zone 1A (except for its trailing edge, which would usually be in Zone 1B). To account for lateral motion of the channel and scatter, the top and bottom surfaces of the wing 18 inches (0.5m) inboard of the tip should also be considered as within the same zones.

(6) Surfaces of the vehicle for which there is a low possibility of direct contact with the lightning arc channel that are not within any of the above zones, but which lie between them, should be considered as within Zone 3. Zone 3 areas must carry substantial amounts of electrical energy.

11. LIGHTNING ENVIRONMENT. For verification purposes, the natural lightning environment (which comprises a wide statistical range of current levels, duration, and number of strokes) is represented by current test Components A through E, and voltage Components A, B, and D (per figures 4, 5 and 6) shown in appendix 2. When testing or analysis are required, the following waveforms should be used. (Applications of waveforms and lightning zones are detailed in appendix 3.)

a. Current Waveforms. There are four current components (A, B, C, and D) that are applied to determine direct effects. Current waveform E is used in tests to determine indirect effects. Components A, B, C, and D each simulate a different characteristic of the current in a natural lightning flash and are shown in figure 4 of appendix 2. They are applied individually or as a composite of two or more components together in one test. The tests in which these waveforms are applied are presented in appendix 3.

(1) Component A - Initial High Peak Current. Component A has a peak amplitude of 200kA ($\pm$10 percent) and an action integral ($\int i^2dt$) of $2\times10^6 A^2$ s ($\pm$20 percent) with a total time duration not exceeding 500 microseconds. This component may be unidirectional or oscillatory. For analysis purposes, a double exponential current waveform should be used. This waveform represents a return stroke of 200,000 amperes peak at a peak rate of rise of 1×10^{11} A/s. This waveform is defined mathematically by the double exponential expression shown below:

$$i(t) = I_o\,(\varepsilon^{-\alpha t} - \varepsilon^{-\beta t})$$

where

I_o = 223,000(A)

α = 11,000 (s^{-1})

β = 460,000 (s^{-1})

t = time(s)

(2) Component B - Intermediate Current. Component B has an average amplitude of 2kA (±10 percent) flowing for a maximum duration of 5 milliseconds unidirectional; e.g., rectangular, exponential, or linearly decaying. For analysis purposes, a double exponential current waveform should be used. This waveform is described mathematically by the double exponential.

$$i(t) = I_o (\epsilon^{-\alpha t} - \epsilon^{-\beta t})$$

$$I_o = 11300(A)$$

$$\alpha = 700 \ (s^{-1})$$

$$\beta = 2000 \ (s^{-1})$$

$$t = \text{time } (s)$$

If the dwell time is more than 5ms, apply an average current of 400A for the remaining dwell time. The dwell time shall have been determined previously through a swept-stroke attachment test or by analysis. If such determination has not been made, the dwell time shall be taken to be 50ms.

(3) Component C - Continuing Current. Component C transfers a charge of 200 coulombs (±20 percent) in a time of between 0.25 and 1 second. This implies current amplitudes of between 200 and 800 amps. The waveform shall be unidirectional: e.g., rectangular, exponential or linearly decaying. For analysis purposes, a square waveform of 200A for a period of 1 sec. should be utilized

(4) Component D - Restrike Current. Component D has a peak amplitude of 100kA (±10 percent) and an action integral of $0.25 \times 10^6 A^2$ s (±20 percent). This component may be either unidirectional or oscillatory with a total time duration not exceeding 500 microseconds. For analysis purposes a double esponential current waveform should be used. This waveform represents a re-strike of 100,000 amperes peak at a peak rate-of-rise of 0.5×10^{11} A/s. The waveform is defined mathematically by the double exponential expression shown below:

$$i(t) = I_o (\epsilon^{-\alpha t} - \epsilon^{-\beta t})$$

$$I_o = 130{,}000 \ (A)$$

$$\alpha = 27{,}500 \ (s^{-1})$$

$$\beta = 415{,}000 \ (s^{-1})$$

$$t = \text{time } (s)$$

(5) Current Waveform E - Fast Rate-of-Rise Stroke Test for Full Size Hardware. Current waveform E has a rate-of-rise of at least 25kA/μs for at least 0.5 microseconds, as shown in figure 4 of appendix 2. Current waveform E has a minimum amplitude of 50kA. Alternatively, components A or D may be applied with a 25kA/μs rate-of-rise for at least 0.5 microseconds and the direct and indirect effects evaluation conducted simultaneously.

i. Indirect effects measured as a result of this waveform must be extrapolated as follows. Induced voltages dependent upon resistive or diffusion flux should be extrapolated linearly to a peak current of 200 kA.

ii. Induced voltages dependent upon aperture coupling should be extrapolated linearly to a peak rate-of-rise of 100 kA/µs.

b. Voltage Waveforms - Test. There are three voltage waveforms, "A," "B," and "D," which represent the electric fields associated with a lightning strike. Voltage waveforms "A" and "D" are used to test for possible dielectric puncture and other potential attachment points. Voltage waveform "B" is used to test for streamers. The tests in which these waveforms are applied are presented in appendix 3.

(1) Voltage Waveform A - Basic Lightning Waveform. Waveform A has an average rate-of-rise of 1×10^6 volts per microsecond ($\pm$50 percent) until its increase is interrupted by puncture of, or flashover across, the object under test. At that time, the voltage collapses to zero. The rate of voltage collapse or the decay time of the voltage if breakdown does not occur (open circuit voltage of lightning voltage generator) is not specified. Voltage waveform A is shown in figure 5 of appendix 2.

(2) Voltage Waveform B - Full Wave. Waveform B rises to crest in 1.2us ($\pm$20 percent). Time-to-crest and decay time refer to the open circuit voltage of the lightning voltage generator, and assume that the waveform is not limited by puncture or flashover of the object under test. This waveform is shown in figure 5 of appendix 2.

(3) Voltage Waveform D - Slow Front. The slow-fronted waveform has a rise time between 50 and 250 microseconds to allow time for streamers from the test object to develop. It should give a higher strike rate in tests to the low probability regions that might have been expected in flight. This waveform is shown in figure 6 of appendix 2.

J. A. Pontecorvo

JOSEPH A. PONTECORVO
Deputy Director, Office of Airworthiness

PURPOSE. For the purposes of this AC, the following definitions apply:

a. Action Integral. The action integral concept is difficult to visualize, but is a critical factor in the production of damage. It relates to the energy deposited or absorbed in a system. However, the actual energy deposited cannot be defined without a knowledge of the resistance of the system. For example, the instantaneous power dissipated in a resistor is by Ohm's Law, $i(t)^2R$, and is expressed in watts. For the total energy expended, the power must be integrated over time to get the total watt-seconds (or kilowatt hours). The watt-second is equivalent to the joule. Without a knowledge of R, we cannot specify the energy deposited. By specifying the integral of $i(t)^2$ over the time interval involved, a useful quantity is defined for application to any resistance value of interest. In the case of lightning, therefore, this quantity is defined as the action integral and is specified as $\int i(t)^2 dt$ over the time the current flows.

b. Attachment Point. A point of contact of the lightning flash with the airplane surface.

c. Average Rate-of-Rise of Voltage. The average rate-of-rise, dv/dt, of a waveform is defined as the slope of a straight line drawn between the points where the amplitude is 30 percent and 90 percent of its peak value.

d. Charge Transfer. The charge transfer is defined as the integral of the time-varying current over its entire duration, $\int i(t)dt$.

e. Corona. A luminous discharge that occurs as a result of an electrical potential difference between the airplane and the surrounding atmosphere.

f. Decay Time of a Voltage Waveform. The decay time of a waveform is defined as the time interval between the intersect with the abscissa of a line drawn through the points where the voltage is 30 percent and 90 percent of its peak value during its rise, and the instant when the voltage has decayed to 50 percent of its peak value.

g. Direct Effects. Physical damage effects caused by lightning attachment directly to hardware or components, such as arcing, sparking, or fuel tank skin puncture.

h. Lightning Attachment. Contact of the main channel of a lightning flash with the airplane.

i. Dwell Time. The period of time that the lightning arc channel remains attached to a single spot.

j. Indirect Effects. The results of electromagnetic coupling from lightning (suoh as induced sparking in fuel quantity probe wiring).

k. Leader. The stepped leader is initiated by a preliminary breakdown within the cloud. The preliminary breakdown sets the stage for negative charge to be channeled towards the ground in a series of short, luminious steps.

l. Lightning Flash. The total lightning event in which charge is transferred from one charge center to another. It may occur within a cloud, between clouds, or between a cloud and ground. It can consist of one or more lightning strokes.

m. Lightning Strike. Any attachment of the lightning flash to the airplane.

n. Lightning Stroke (Return Stoke). A lightning current surge, return stroke, that occurs when the lightning leader makes contact with the ground or another charge center.

o. Streamering. The branch-like ionized paths that occur in the presence of a direct stroke or under conditions when lightning strokes are imminent.

p. Swept-Stroke. A series of successive attachments due to sweeping of the flash across the surface of the airplane by the motion of the airplane.

q. Time-to-Crest of a Voltage Waveform. The time-to-crest of a waveform is defined as 1.67 times the time interval between the instants when the amplitude is 30 percent and 90 percent of its peak value.

r. Time Duration of a Current Waveform. The time duration of a current waveform is defined as the time for initiation of current flow until the amplitude (peak amplitude in the case of a damped sinusoid) has reduced to 5 percent of its initial peak value.

T_0 - Initial Attachments

T_{1-5} Subsequent Attachments

T_n - Final Attachment Points

(LIGHTNING CHANNEL POSITION SHOWN RELATIVE TO AIRPLANE)

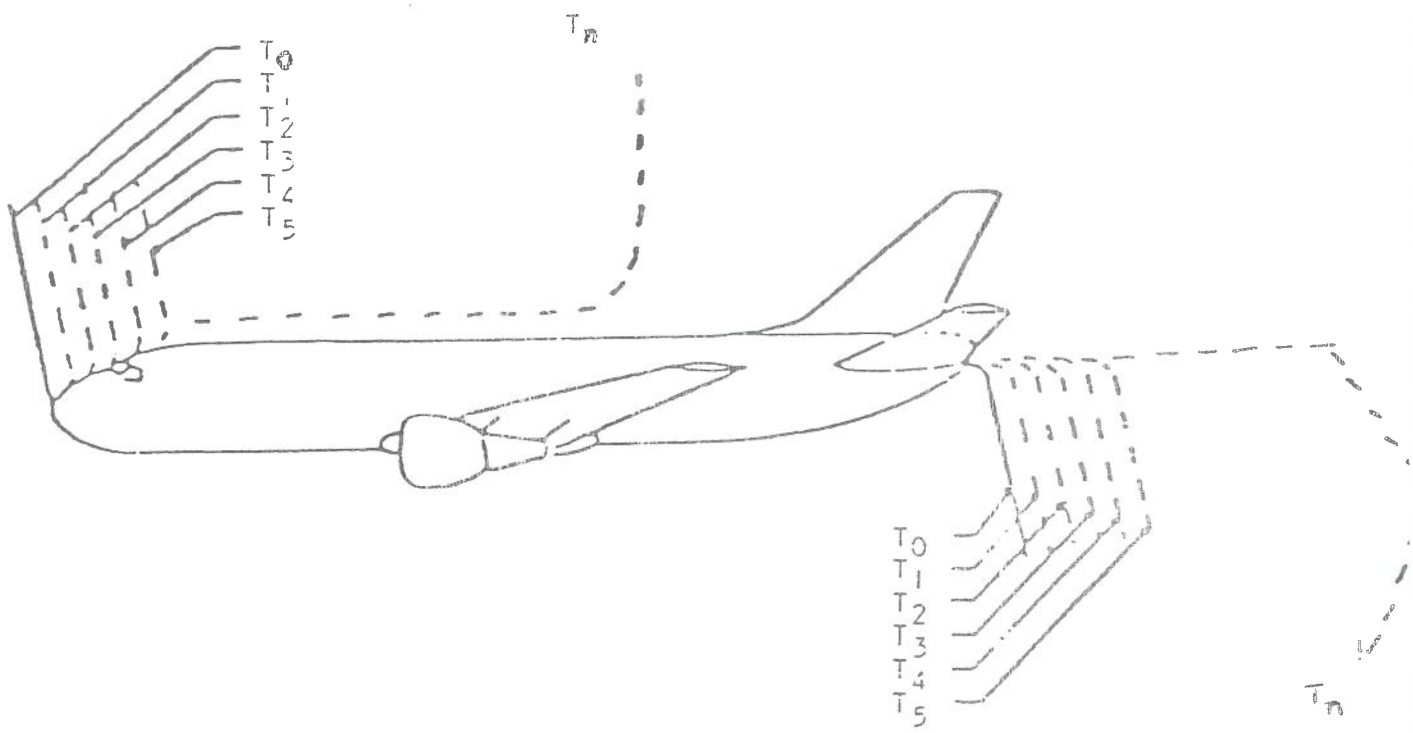

FIGURE 1 - SWEPT-STROKE PHENOMENON

LIGHTNING STRIKE ZONES

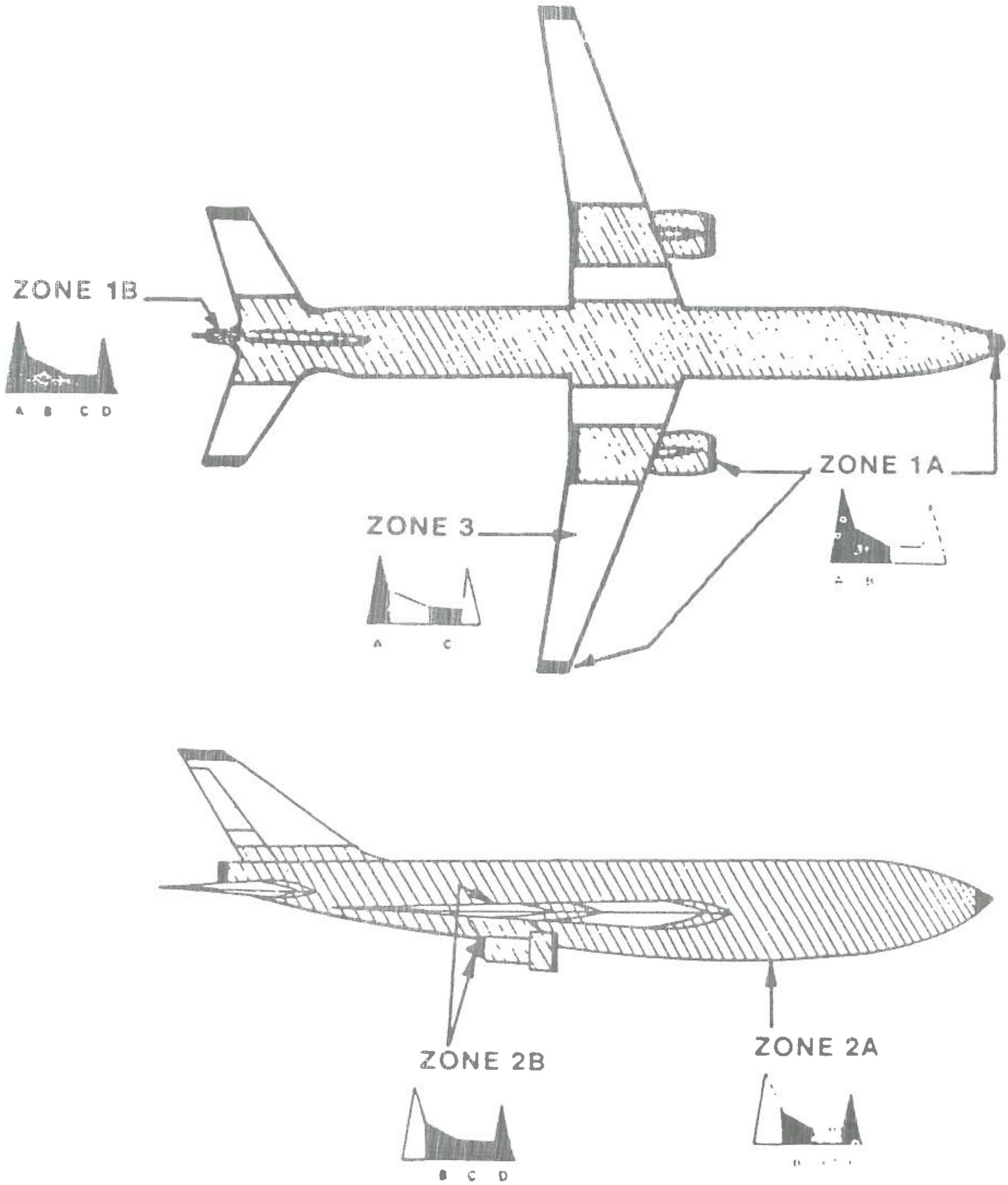

FIGURE 2 LIGHTNING STRIKE ZONES (TYPICAL)
(See paragraph 10C)

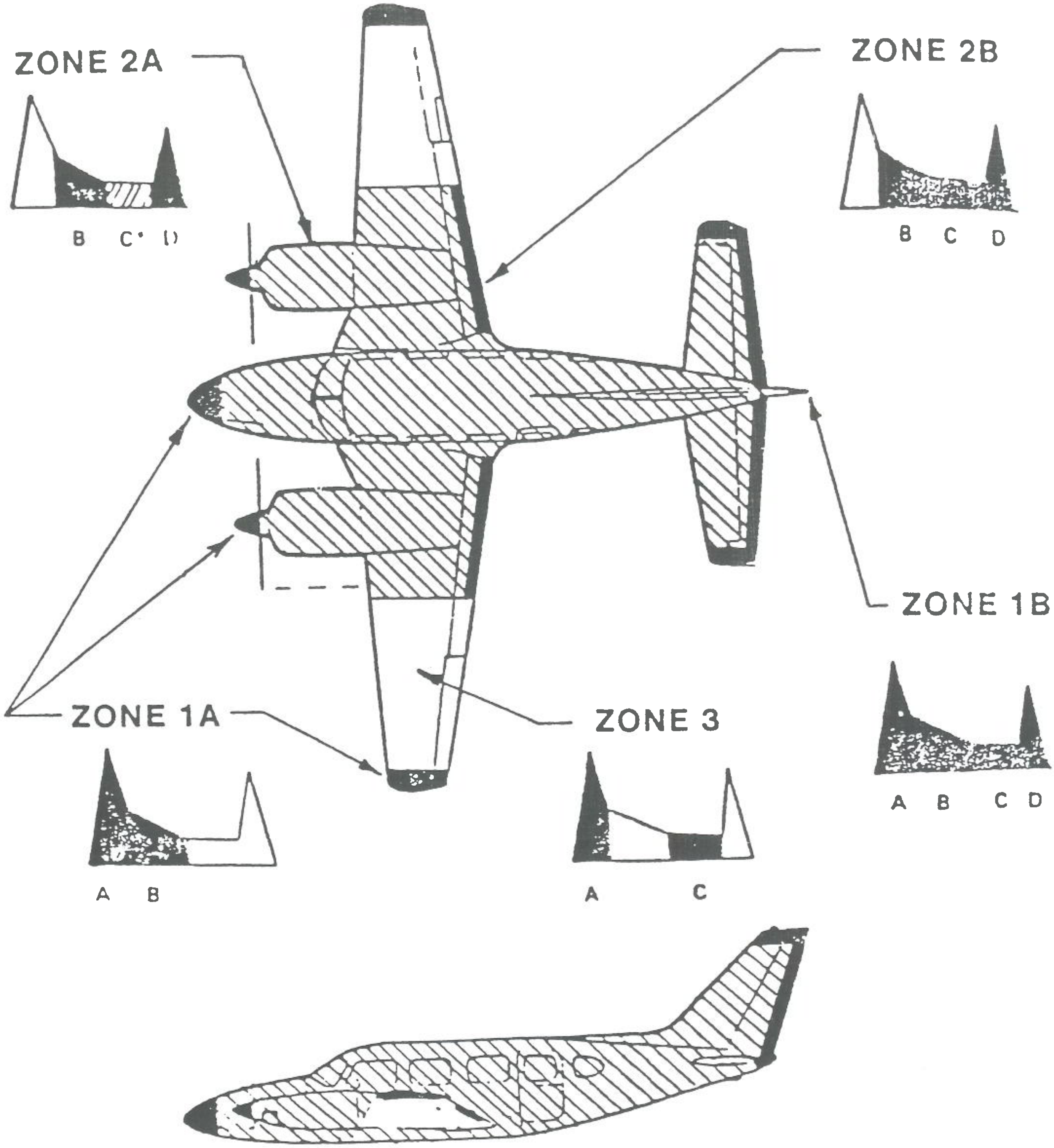

FIGURE 3 LIGHTNING STRIKE ZONES (TYPICAL)
(See paragraph 10C)

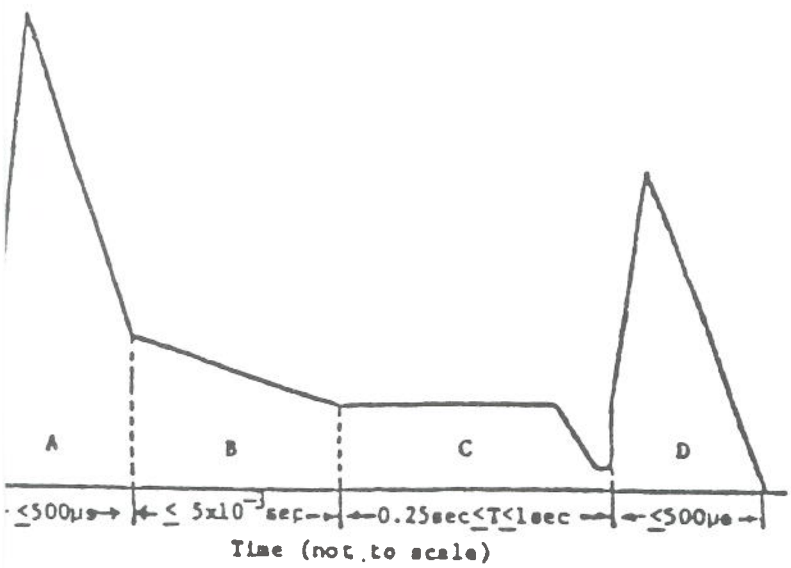

COMPONENT A (Initial Stroke)
Peak Amplitude = 200kA (±10%)
Action Integral = $2\times10^6 A^2s$ (±20%)
Time Duration = ≤500 μs

COMPONENT B (Intermediate Current)
Maximum Charge Transfer = 10 Coulombs
Average Amplitude = 2kA (±10%)

COMPONENT C (Continuing Current)
Charge Transfer = 200 Coulombs (±20%)
Amplitude = 200-800A

COMPONENT D (Restrike)
Peak Amplitude = 100kA (±10%)
Action Integral = $0.25\times10^6 A^2s$ (±20%)
Time Duration = ≤500 μs

COMPONENTS A THROUGH D WAVEFORMS

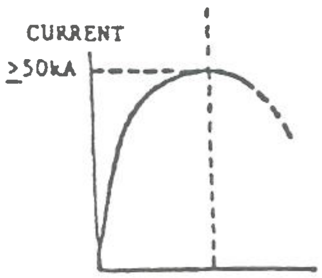

COMPONENT WAVEFORM E
Peak Amplitude = ≥ 50kA
Rate of Rise = ≥ 25kA/μs
for at least 0.5μs

FIGURES NOT TO SCALE

Rate of Current Rise

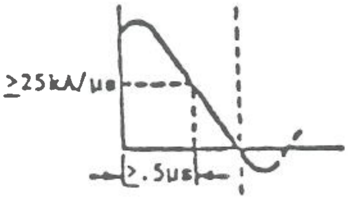

Definition of rate
of rise requirement
of waveform E

FIGURE 4 CURRENT WAVEFORMS

4

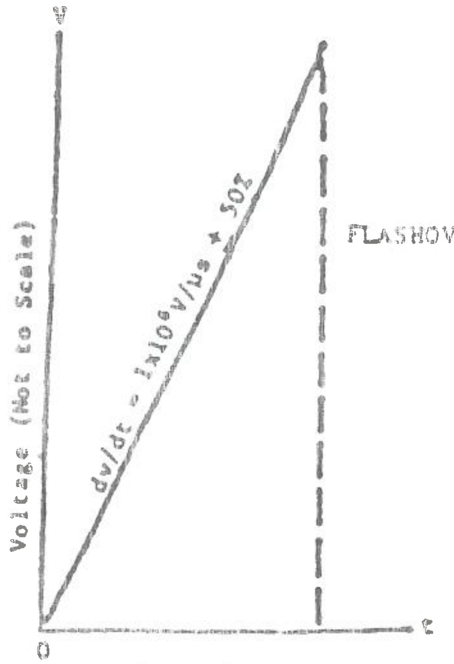

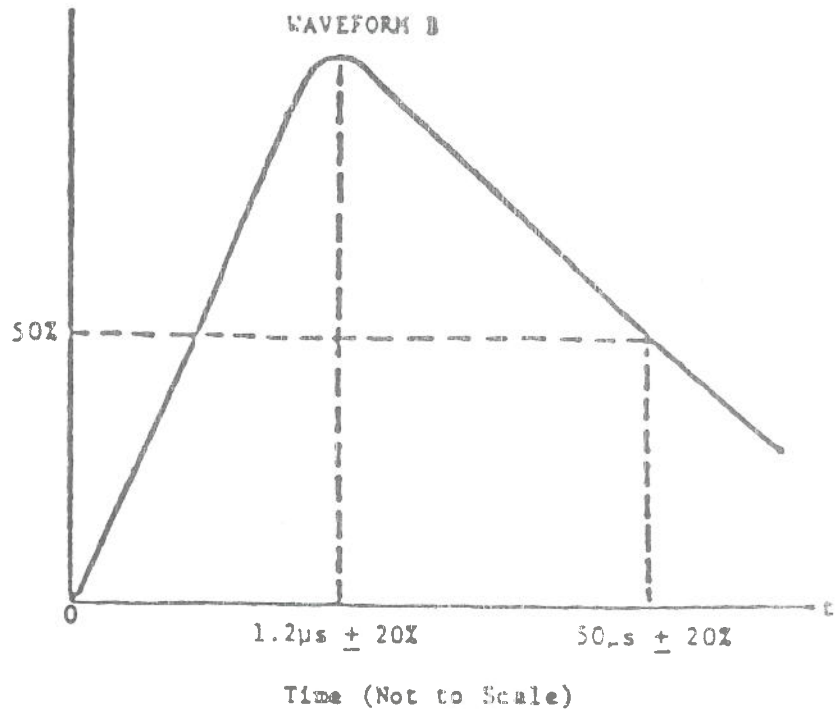

NOTE: Voltage Waveform "B" Full Wave - Waveform "B" rises to crest in 1.2 µs (±20 percent). Time-to-crest and decay time (refer to open circuit voltage) of the lightning voltage generator, and assume that the waveform is not limited by puncture or flashover of the object under test.

FIGURE 5 VOLTAGE WAVEFORMS 'A'&'B'

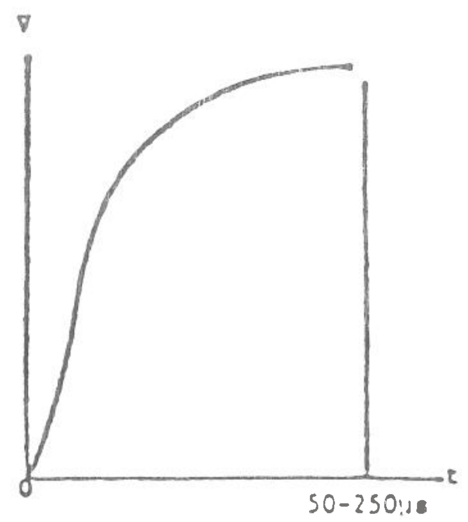

FIGURE 6 VOLTAGE WAVEFORM 'D'

APPLICATION OF WAVEFORMS FOR LIGHTNING TESTS

Test	Zone	Voltage A	Voltage B	Voltage D	Current Components A	Current Components B	Current Components C	Current Components D	Current Components E
Full Size Hardware Attachment Point	1A, 1B	X		X[1]					
Direct Effects Structural	1A				X	X			
	1B				X	X	X	X	
	2A					X[2]	X[2]	X	
	2B					X	X	X	
	3				X		X		
Direct Effects Combustible Vapor Ignition	1A				X	X			
	1B				X	X	X	X	
	2A					X[2]	X[2]	X	
	2B					X	X	X	
	3				X		X		
Direct Effects Corona and Streamers			X						
Indirect Effects Related to Spark Generation Within Fuel Vapor Areas									X[3]

NOTE 1: Voltage waveform "D" may be applied to identify lower probability strike points.

NOTE 2: Use an average current of 2kA ± 10 percent for a period equal to the dwell time up to a maximum of 5ms. If the dwell time is more than 5ms, apply an average current of 400A for the remaining dwell time. The dwell time shall have been determined previously through a swept-stroke attachment test or by analysis. If such determination has not been made, the dwell time shall be taken to be 50ms.

NOTE 3: Indirect effects should also be measured with current components A, B, C, or D as appropriate.

Extracts from LTT report AEA-TSD-0562

7 TEST WAVEFORMS

7.1 Requirement

The blades were to be tested at levels up to, including and in excess of the Zone 1A lightning certification test level specified in Reference 3, and summarised below.

COMPONENT A (Initial Attachment):	Peak Current = 200kA ±10% Action Integral = $2 \times 10^6 A^2s$ ±20% Duration = ≤500μs.
COMPONENT B (Intermediate Current):	Average Current = 2kA ±10% Charge Transfer = 10C Duration 5ms.
COMPONENT C_1 (Continuing Current): *Also known as Short C*	Current Amplitude = 400A Charge Transfer = 18C Duration 45ms.

The three components defined above were applied as a single composite pulse in the order A + B + C_1. The C_1 employed will represent a severe case at the initial attachment point to one TRB, the following TRBs will sweep through the lightning arc every 12ms. The total charge transfer to a single blade could be up to one fifth (5 blades) of the charge transfer available in Zone 1B ($^1/_5$ of 200C = 40C), but it is unlikely to have all the charge transferred through the same attachment point.

7.2 Generators

Component A was generated by the LTT A/D Bank, which comprises a two stage 387.5μF capacitor bank that can be charged to a maximum of 40kV/stage.

The current output waveform of the A/D bank is a unidirectional double exponential whose characteristics are modified by varying the inductance and resistance in the generator/load circuit.

Components B + C_1 (also known as Short C) were produced as a single composite pulse from the LTT Slow Bank. This facility comprises three separate capacitor banks (1000μF, 1000μF and 840μF) which can be connected in any parallel combination and charged to a maximum of 18kV. As ignitrons are used in the discharge circuit, the natural current output waveform of the slow bank is a single half cycle. The shape of the slow bank output waveform is modified by introducing external resistors and air cored inductors. Ignitrons were also used to clamp the waveform producing an extended pulse giving a higher charge transfer.

7.3 Diagnostics

The output waveform of the A/D Bank was monitored by a Rogowski coil looped around the output return (low potential) transmission line. The output waveform of the Slow Bank was monitored by a coaxial shunt mounted in the return (low potential) transmission line.

Screened balanced twin cable was used to transmit the output from the Rogowski coil and the shunt to a screened diagnostic room where the signals were processed, stored and digitally displayed. Further digital processing produced the values of peak current, action integral and charge transfer associated with each test.

Typical test current waveforms associated with these tests are reproduced in Appendix II of this report, where waveform analysis methods are also discussed.

7.4 Calibration Status

The current diagnostic measurement systems associated with the A/D and slow capacitor banks are calibrated in accordance with LTT QA procedures.

7.5 Additional Current Measurements

In addition to the bank discharge current measurements described above, two additional Rogowski current measurement coils were used to monitor the current distribution in the blade root/sleeve region. Primarily the aim was to establish the proportion of current flowing off the TRB via the bonding braid. This measurement could only be made at low current levels, as at high current levels the bonding braid was destroyed and there would have been a risk of direct arc attachments to the Rogowski coils.

Both coils and their associated data transmission, processing and display channels were calibrated against the A/D bank system in advance of the test series. The location of these coils and their corresponding measurements are included in the test results presented in Section 14 of this document.

8 THE TEST ASSEMBLY

8.1 General

The parallel plate return conductor assembly shown in Plate 1* was used for these tests. This configuration simulates the free space conditions encountered in flight and therefore gives a representative current distribution in the test blade.

The test blade was mechanically supported by an insulating cradle at a point approximately 150mm in from the outboard tip, and at the blade root by the sleeve and spindle assembly which was bolted to the return conductor assembly.

The return conductor assembly was connected to the low potential (earthy) output terminations of the generators.

An adapter plate was fitted to the high potential output termination of the generator and positioned between the parallel plates in line with the blade. This plate allowed both solid and open arc current injection techniques to be used.

In order to minimise the possibility of any liberated carbon fibre or other conductive debris from compromising the high voltage operation of the test facility, polythene sheets were used to shroud the open sides of the test assembly.

* Figure 1A in this Appendix(C)

Component A Waveform

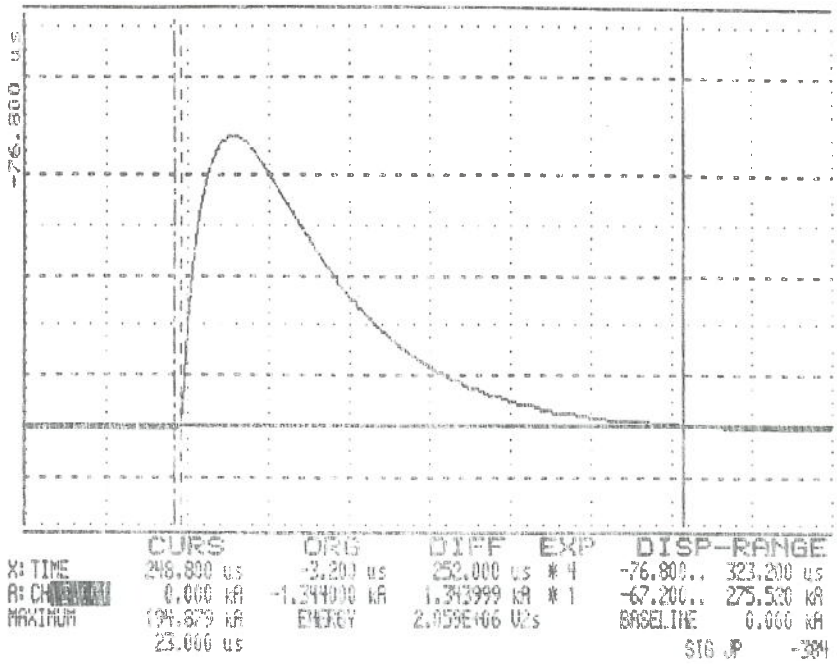

Peak Current is the current amplitude of the positive peak of the waveform.

Action Integral is the integral of the instantaneous current squared (with respect to time) for the duration of the pulse.

NOTE: The bottom line of printed information below the waveform gives the values of Peak Current in kA (MAXIMUM) and the Action Integral in V^2s (ENERGY). The numerical value for the action integral is correct, however the dimensions should be read as A^2s.

Component B and C_1 Waveform.

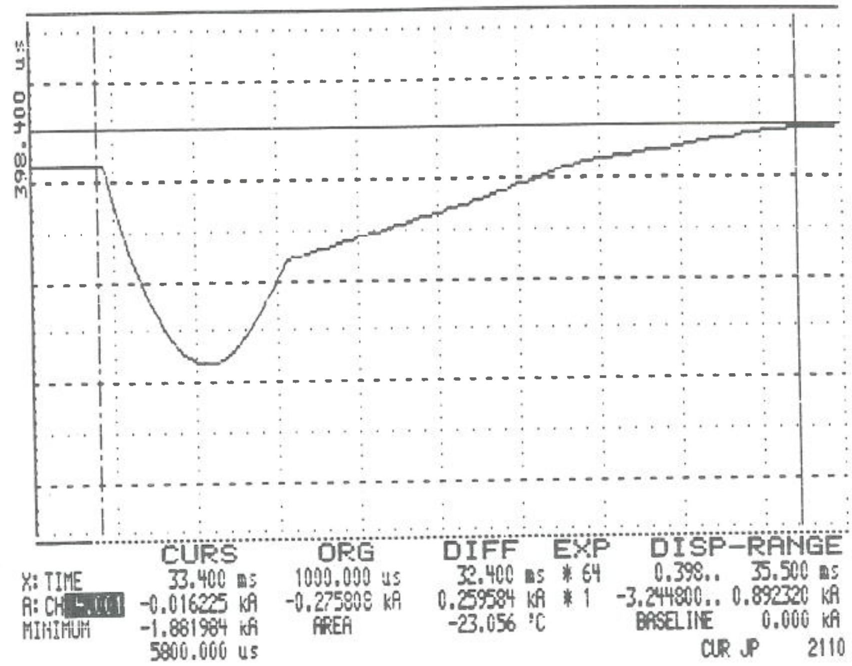

Peak Current (B) - is the current amplitude at the first negative peak of the waveform.

Peak Current (C_1) - is the current amplitude at the instant that clamping occurs and the di/dt of the waveform suddenly drops.

Charge Transfer (B) - is the integral of the instantaneous current (with respect to time) in that part of the waveform preceding Peak Current (C_1).

Charge Transfer (C_1) - is the integral of the instantaneous current (with respect to time) between peak current (C_1) and its subsequent decay to zero.

NOTE: The bottom line of printed information below the waveform gives the values of Peak Current in kA (MINIMUM) and the Charge Transfer in C.

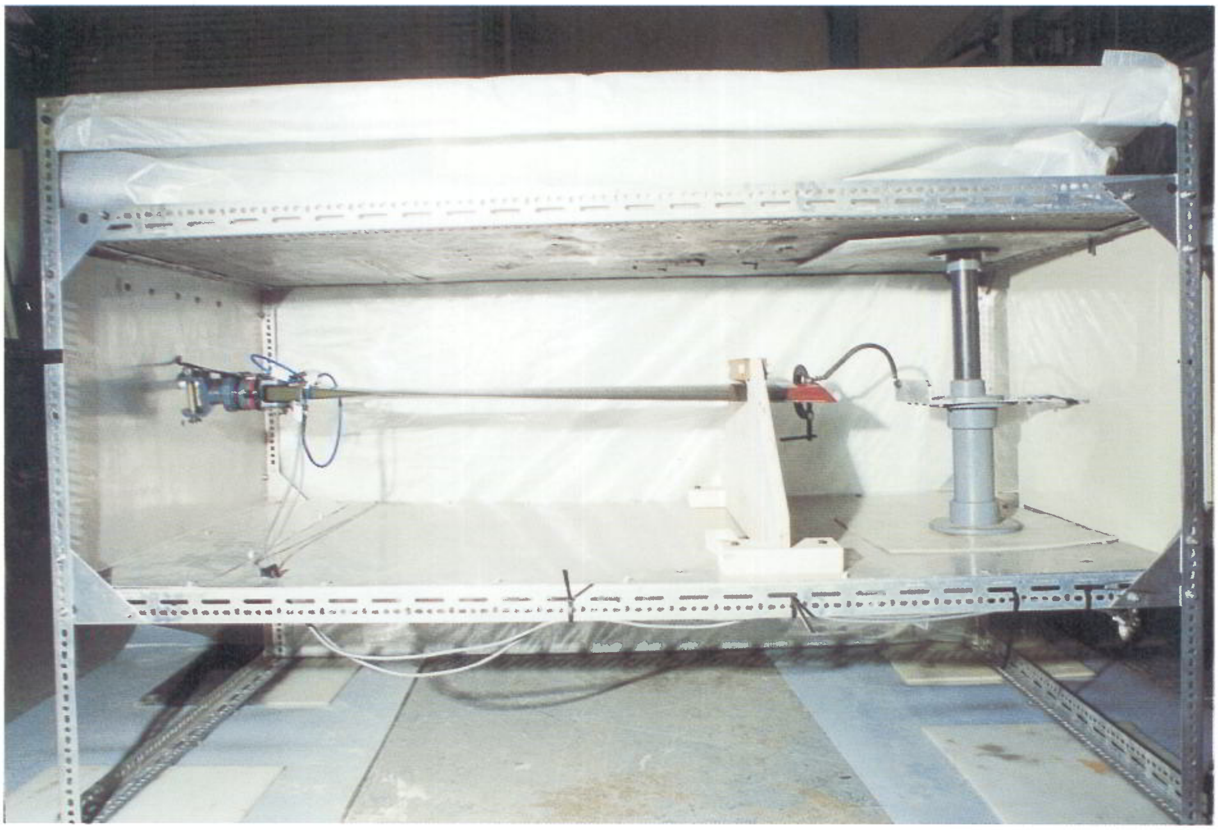

Figure 1A: Showing LTT test cell used for simulated lightning strikes on sample tail rotor blades, as described earlier in Enclosure 2, section 8.1.

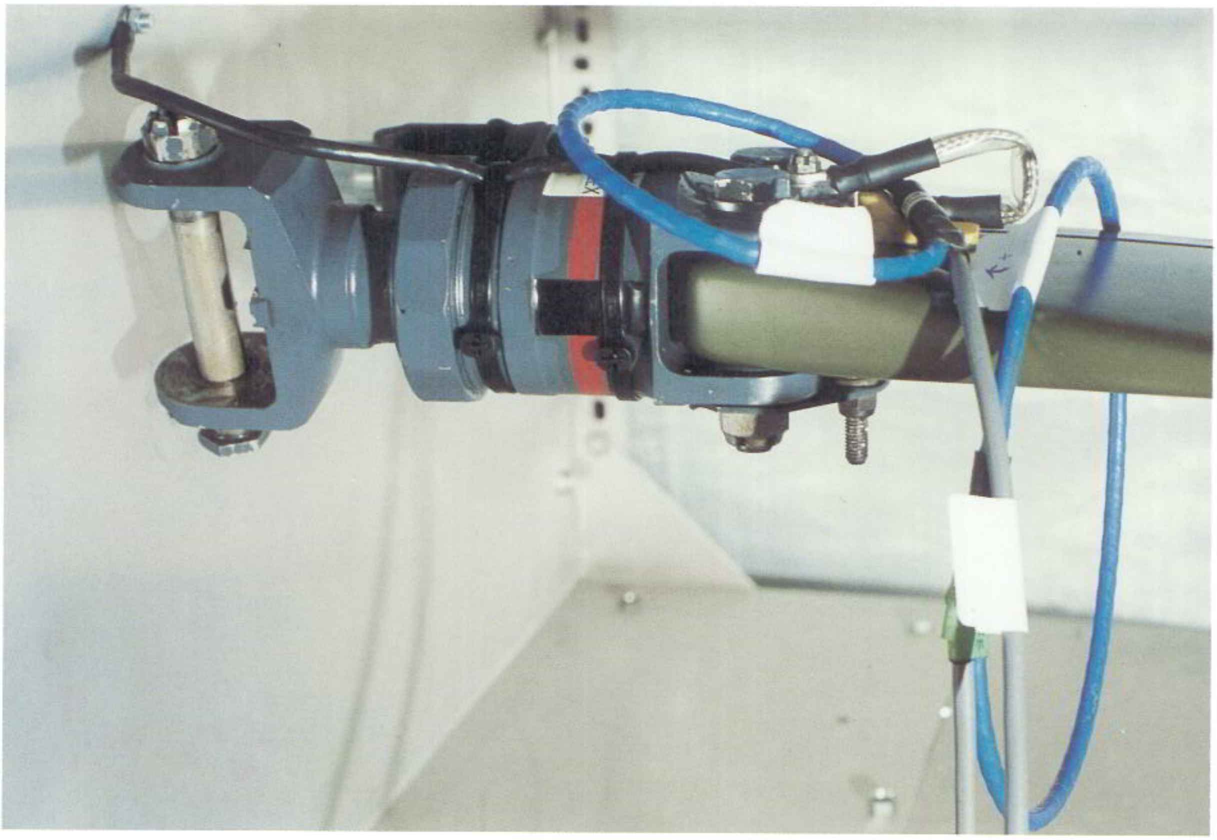

Figure 1B: Showing first test blade with inboard bonding strap and sleeve bolted to metal end plate, and Rogowski coils in position around root area.

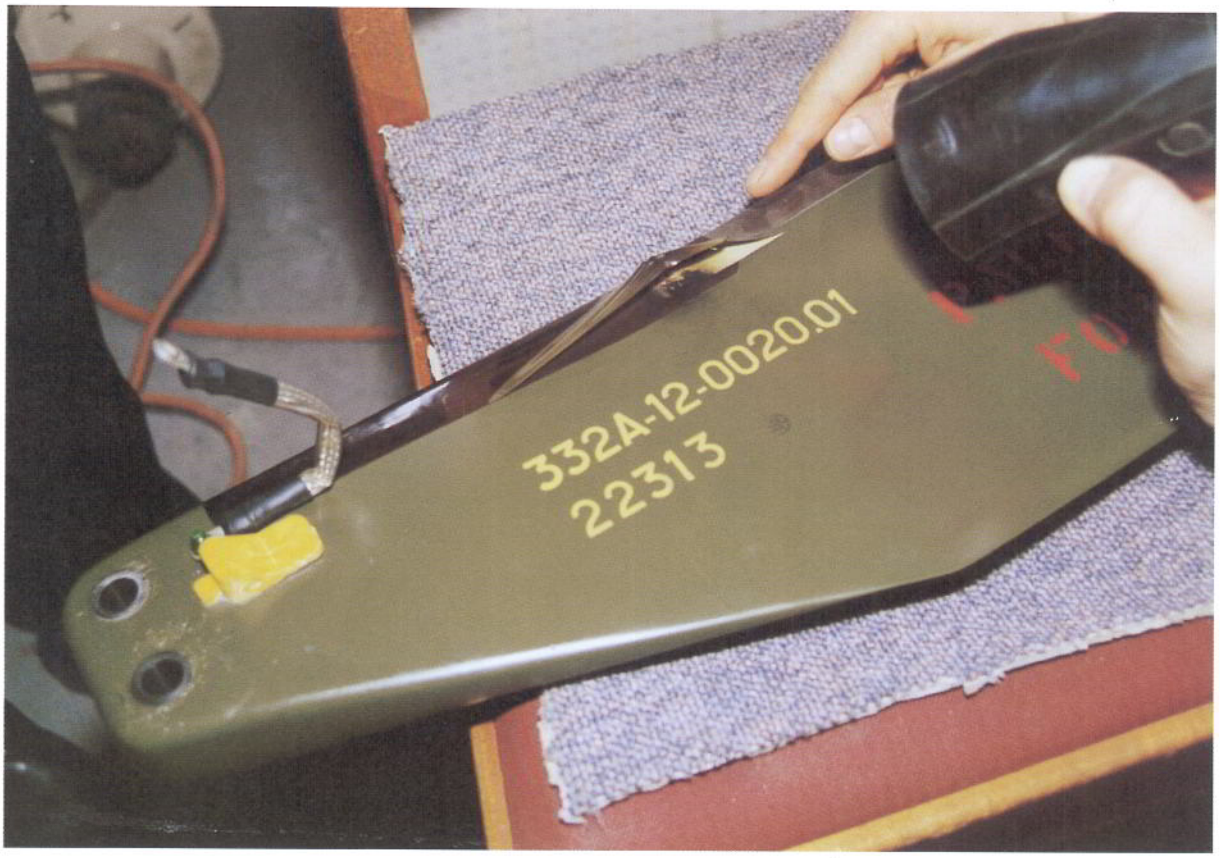

Figure 2: Showing 'peel-back' of inboard end of anti-erosion shield from brass conducting strip after 12.7kA low energy test (shield tip input).

Figure 3: Showing post-test damage to inboard span of TRB s/n 22200 after 190.9kA input to shield tip, with White TRB section for comparison.

Figure 4: Showing tip damage to TRB s/n 20667 after 180.1kA input to trailing edge tip, with peel-back and general debonding of erosion shield.

Figure 5: Showing tip damage to TRB s/n 21667 after 253.7kA input to trailing edge tip, with debonding of erosion shield and 'burn-holes'.

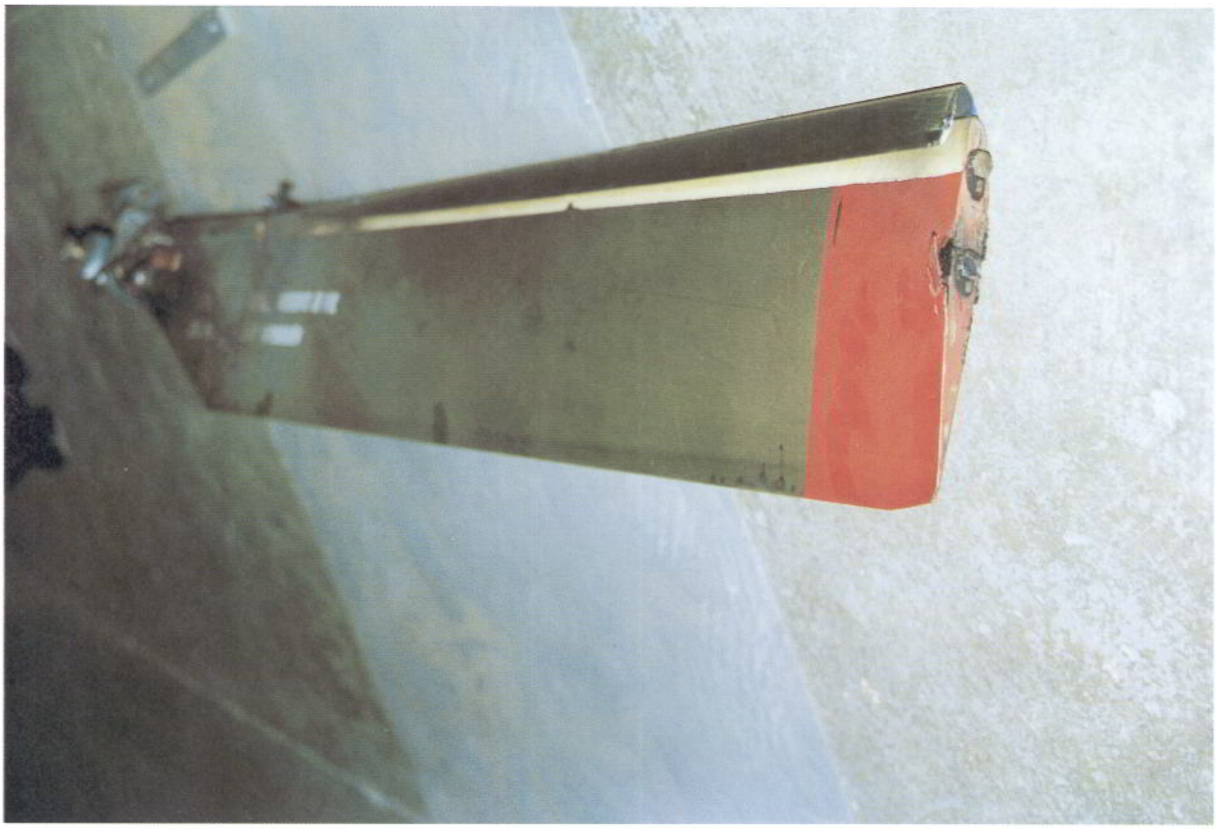

Figure 6A: Showing TRB s/n 20636 after 198.9kA input to aft tip bolt with minor damage around bolt, but almost complete separation of shield.

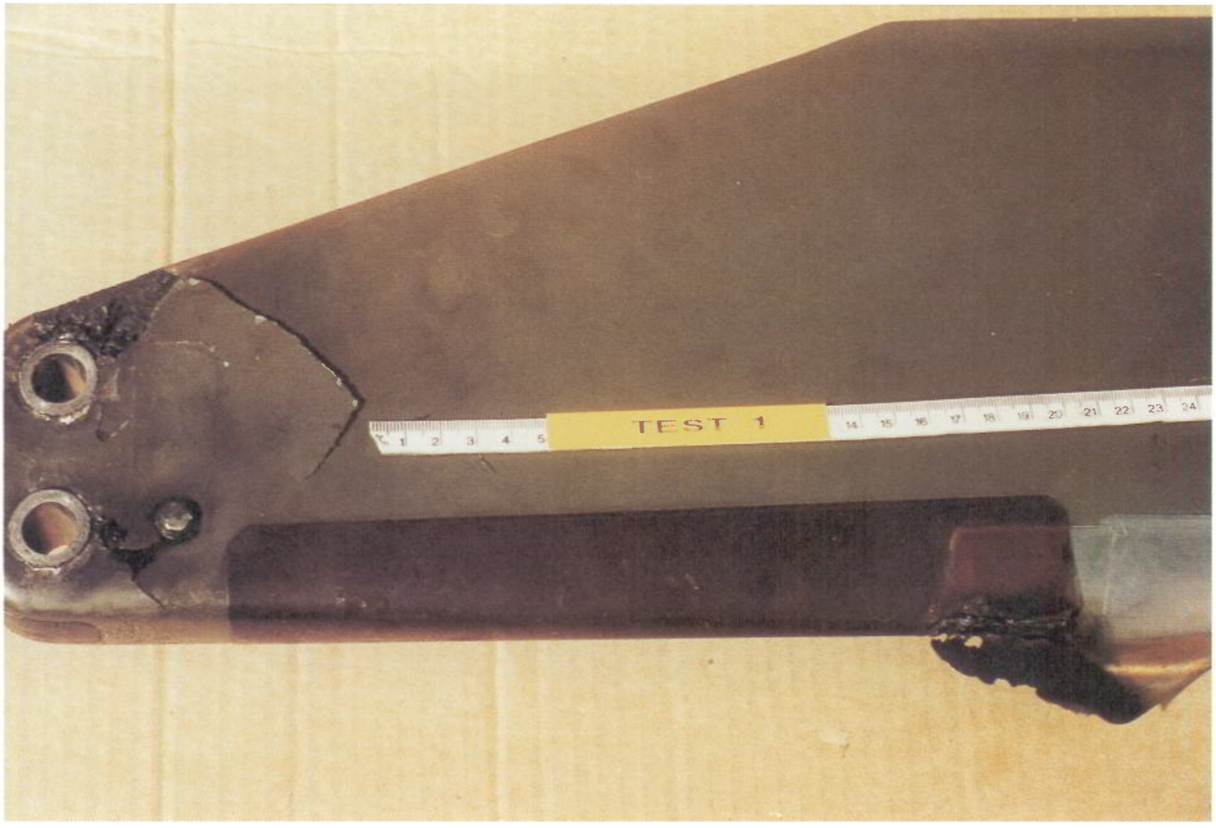

Figure 6B: Showing thermal delamination damage to root area of above TRB.

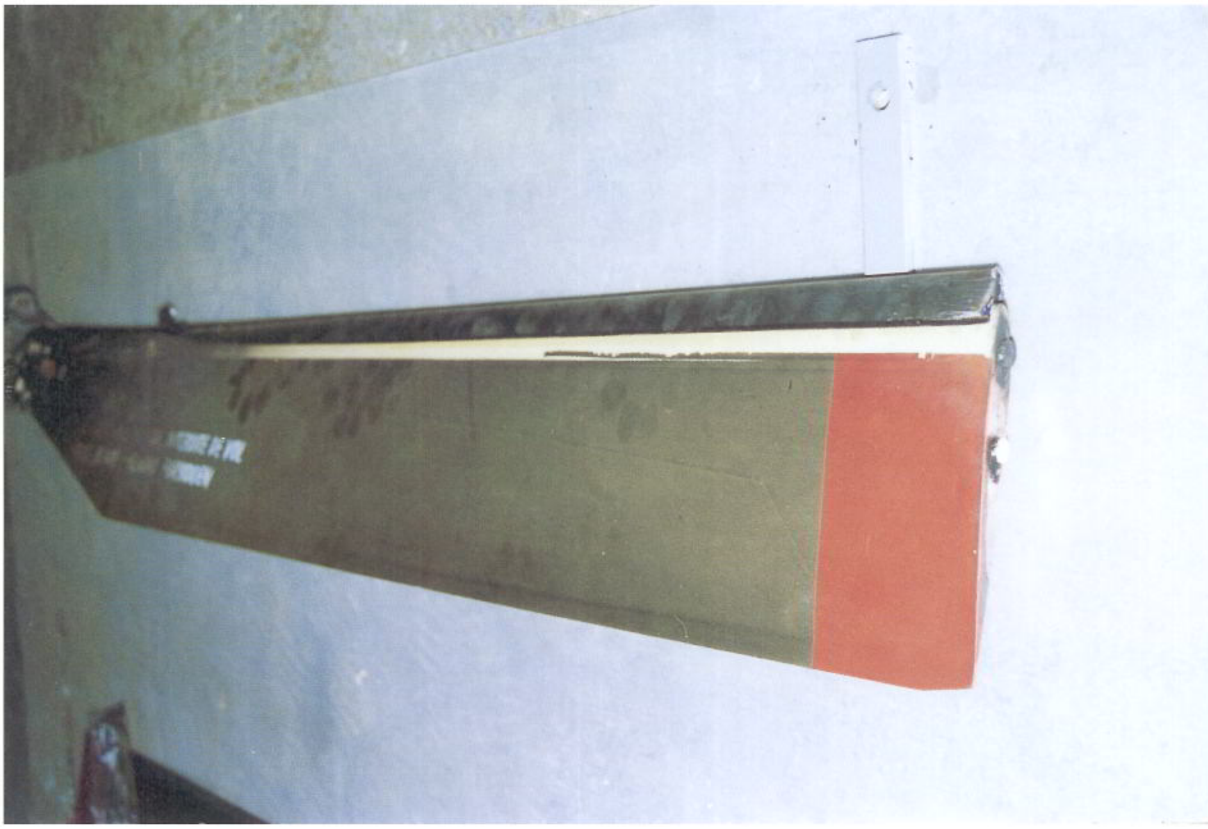

Figure 7A: Showing TRB s/n 20625 after 194.9kA input to forward tip bolt with minor damage around bolt and to erosion shield tip, but almost complete separation of shield.

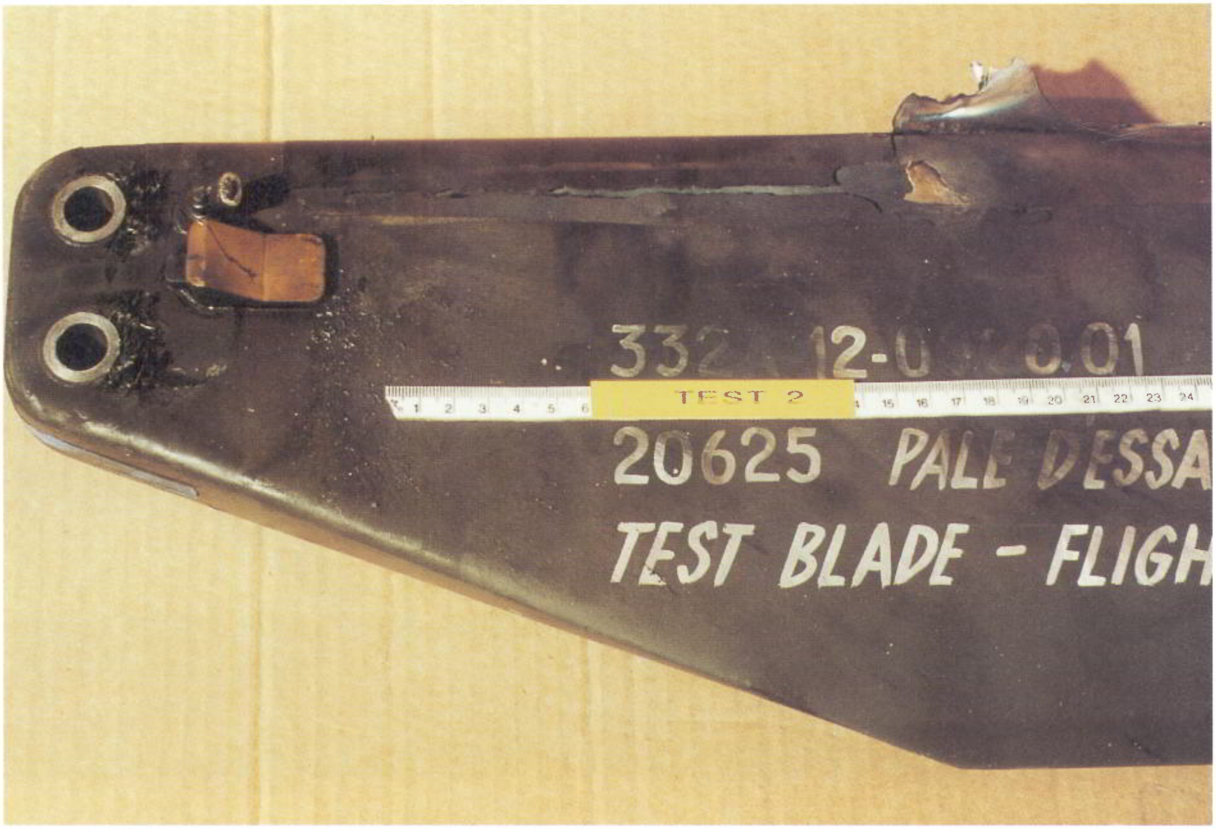

Figure 7B: Showing damage to inboard area of above TRB.

Figure 8A: Showing general marked damage to TRB s/n 20646 after 188.2kA input to trailing edge, 0.5 metre from tip.

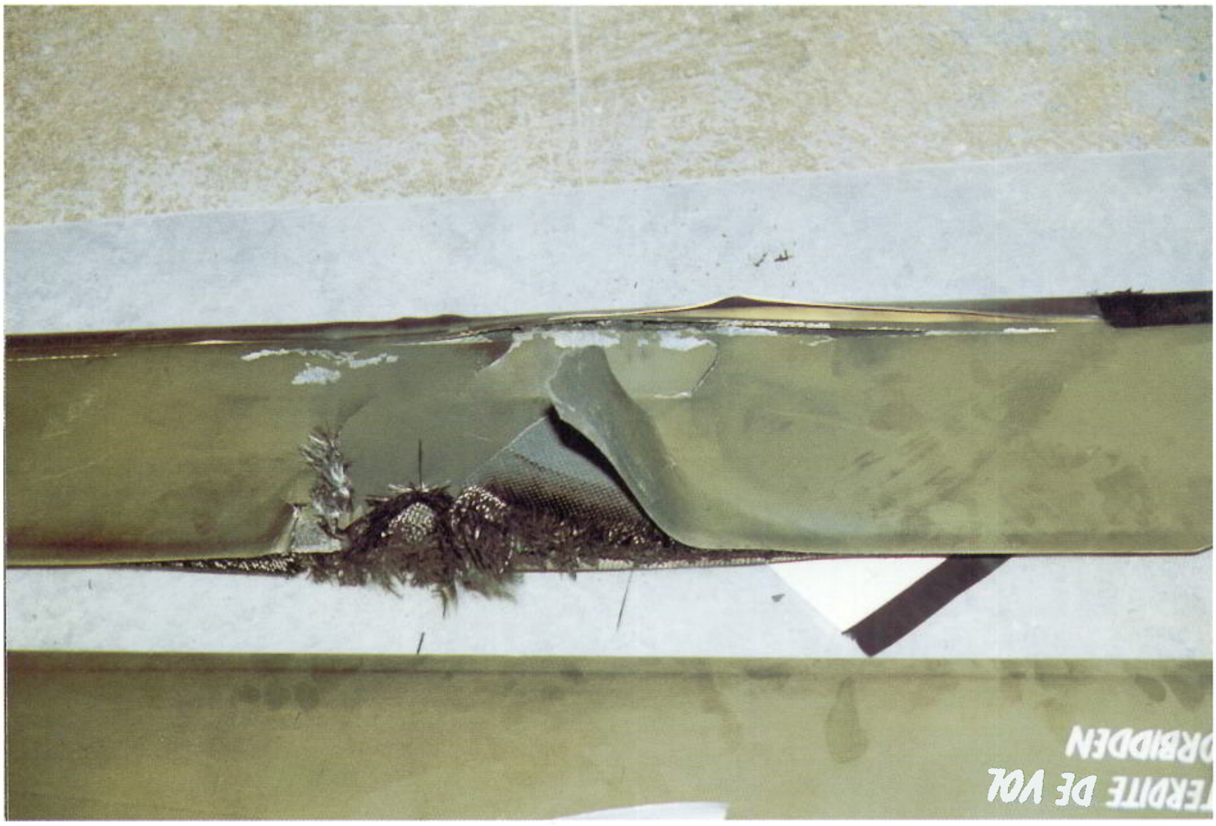

Figure 8B: Showing gross disruption of mid-aerofoil on above TRB and spanwise cracking of skins just aft of erosion shield.

Figure 9A: Showing damage to TRB s/n 20732 after 206.9kA input to inboard end of erosion shield, with local peel-back of shield.

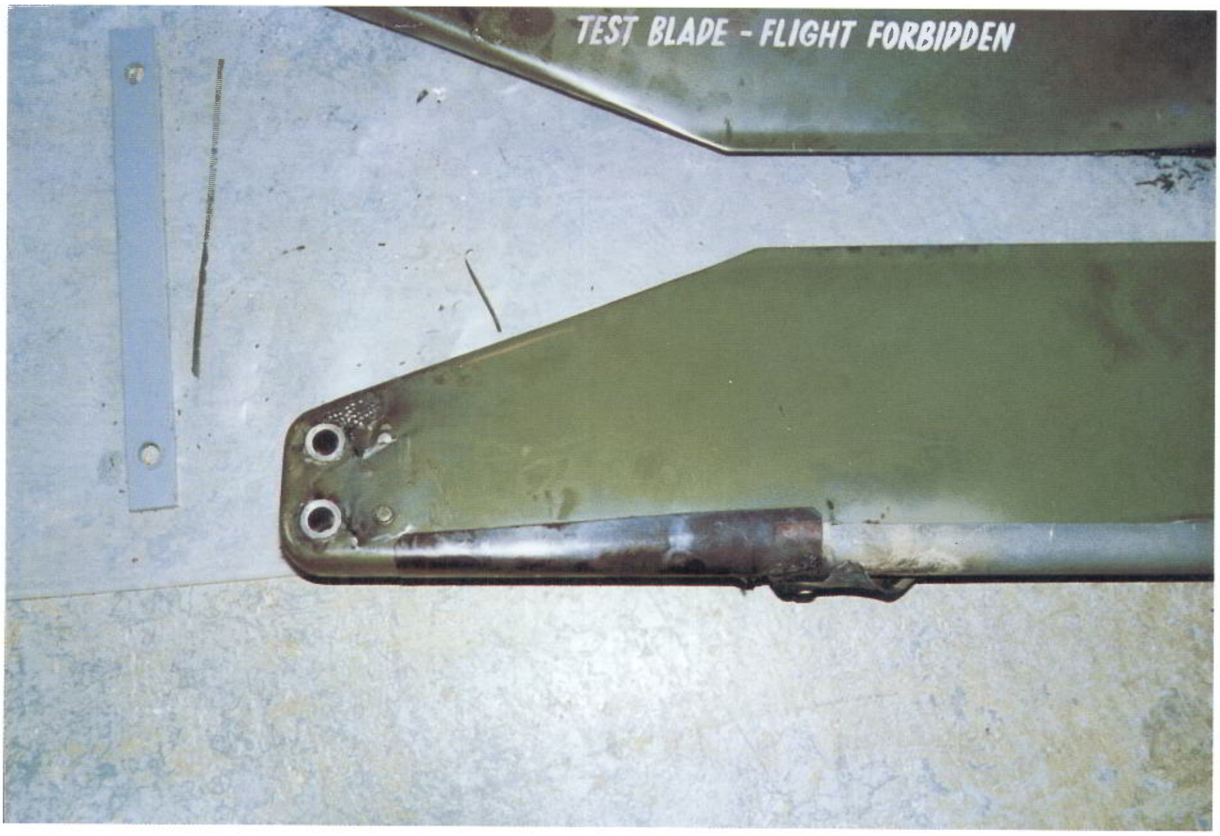

Figure 9B: Showing skin delamination and disbonding outboard of both steel bushes in root area (inboard side) of above TRB.

Figure 10A: Showing detached and badly deformed erosion shield after 275.5kA input to aft tip bolt on TRB s/n 20662.

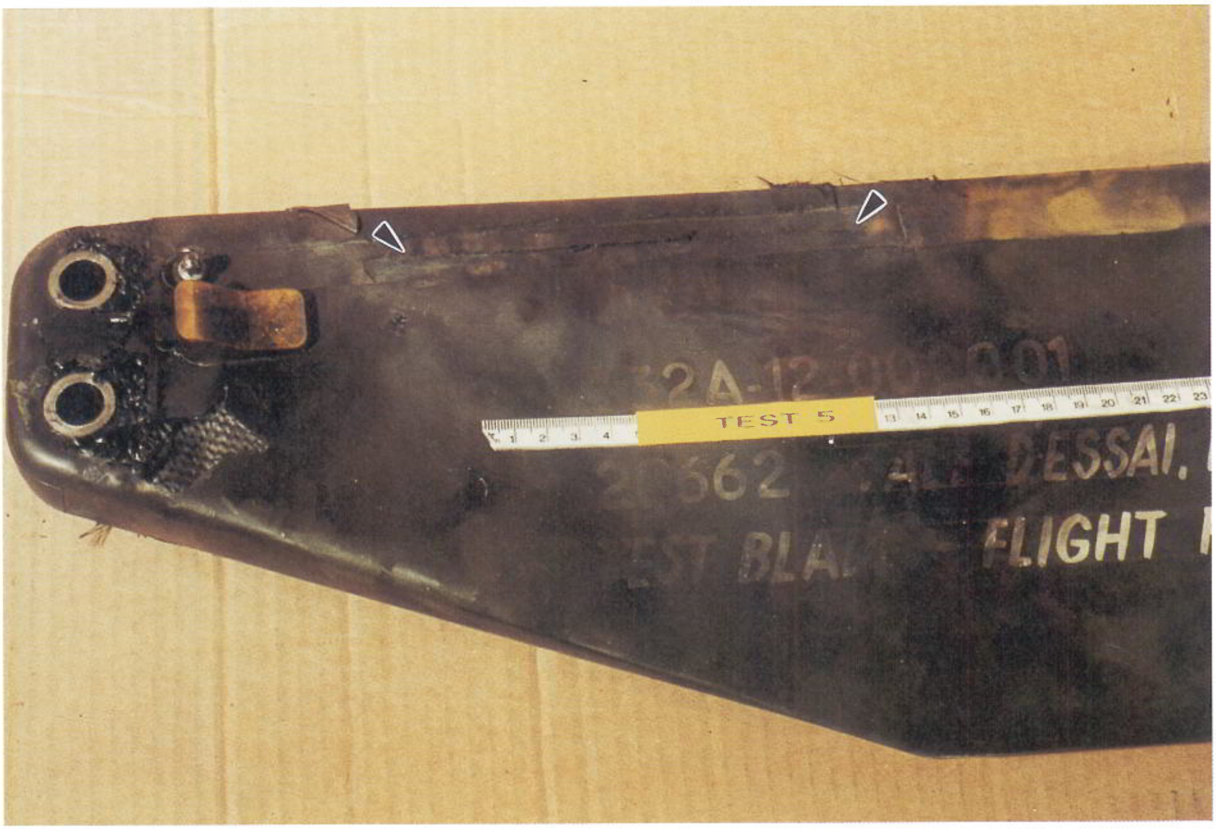

Figure 10B: Showing longitudinal 'fissure'(arrowed) within blade substrate uncovered by loss of brass bonding strip, and root damage on above TRB.

Figure 10C: Showing marked delamination and disbonding of inboard(left) surface of the root of TRB s/n 20662 after 275.5kA input to aft tip bolt.

Figure 11A: Showing gross damage to aerofoil of TRB s/n 22313 after 253.3kA input to trailing edge, 34cm from tip.

Figure 11B: Showing localised damage to leading edge composite and detached inboard length of shield, with 'burn-holes', on above blade.

Figure 11C Showing marked thermal affects on outboard side of root on TRB s/n 22313 with carbon fibre damage adjacent attachment bolts.

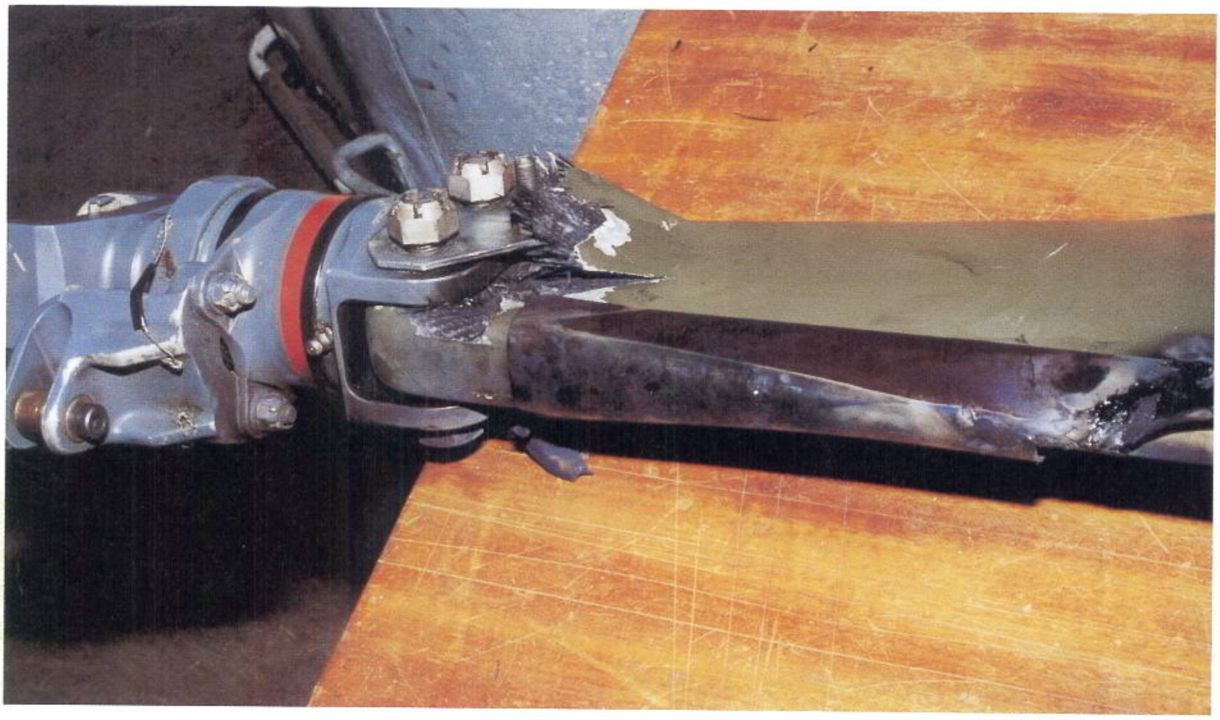

Figure 11D: Showing very marked carbon fibre disbonding and delamination adjacent attachment bolts on inboard side of above blade.

Figure 12A Figure 12B

Showing (Figure 12A) gross damage to aerofoil with (Figure 12B) 'split' in leading edge and detached erosion shield lying alongside TRB s/n 20697 after 253.8kA input to trailing edge, 20cm from tip.

Figure 12C: Showing almost full length 'fissure'(between arrows) within substrate uncovered by loss of brass conducting strip, and root damage adjacent attachment bolt bushes on TRB s/n 20697.

Figure 12D: Showing thermal disbonding and delamination damage to inboard side of root adjacent bushes on TRB s/n 20697.

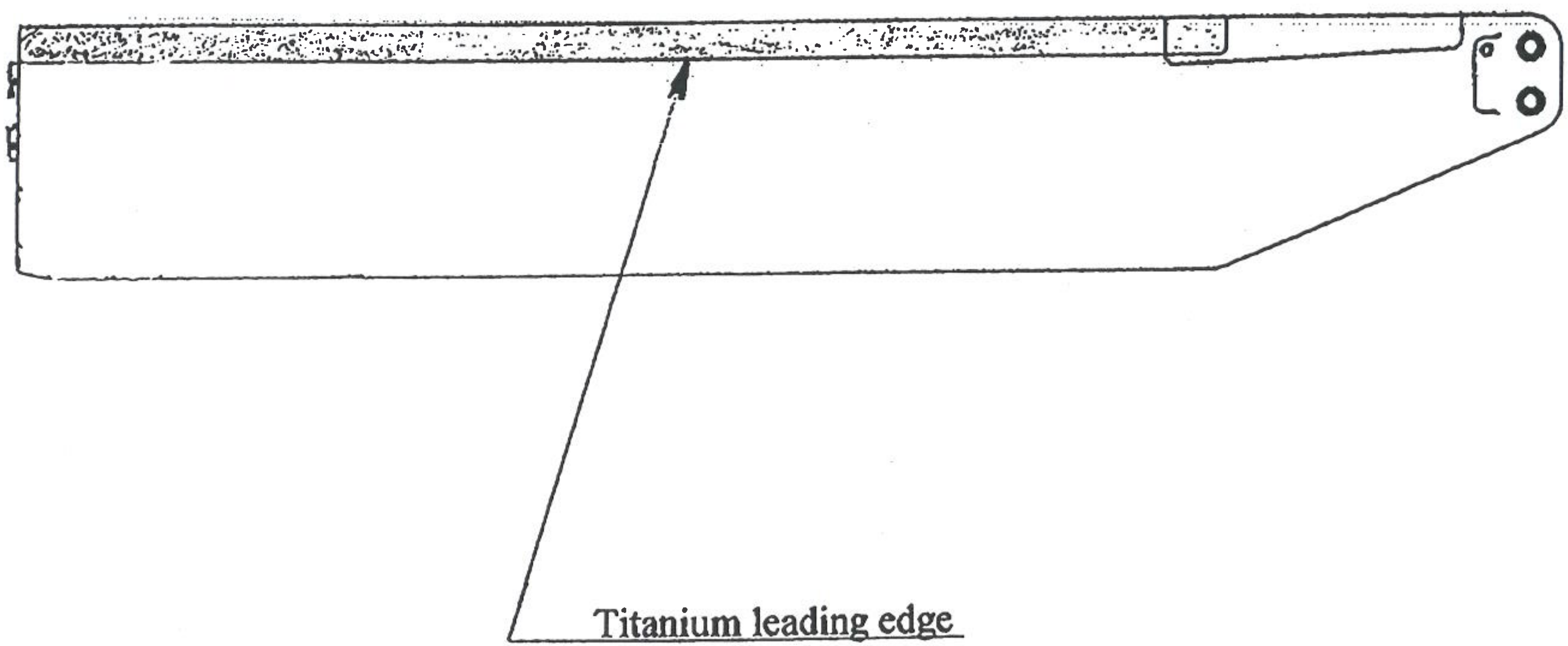

Figure 13A: Showing leading edge anti-erosion shield/conductor design on TRB p/n 332A.12.0020 before modification to improve lightning protection.

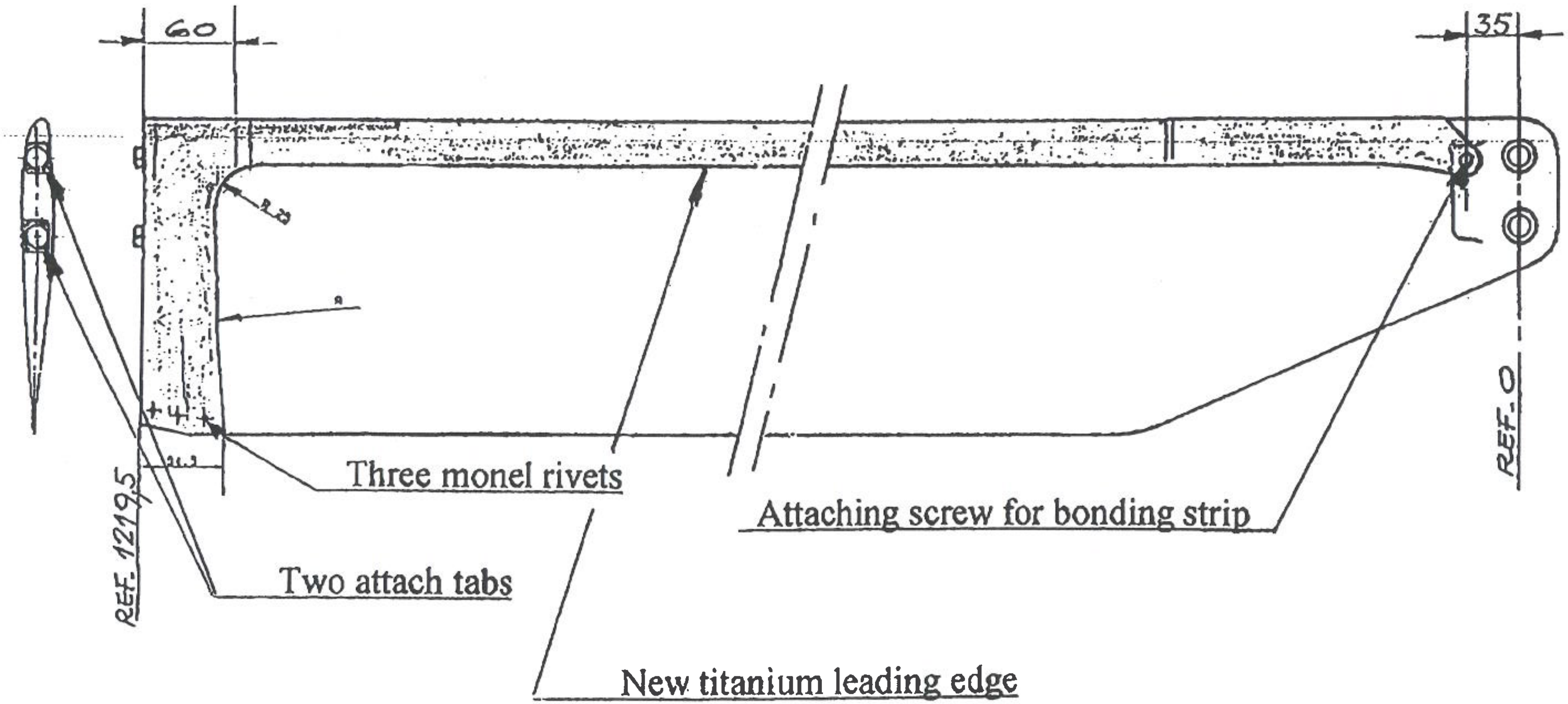

Figure 13B: Showing modified blade p/n 332A.12.0050 design with anti-erosion shield/conductor extended inboard to root and aft to provide improved blade tip conduction, with titanium 'tab' continuity to both tip weight bolts and rivetted attachment to trailing edge.

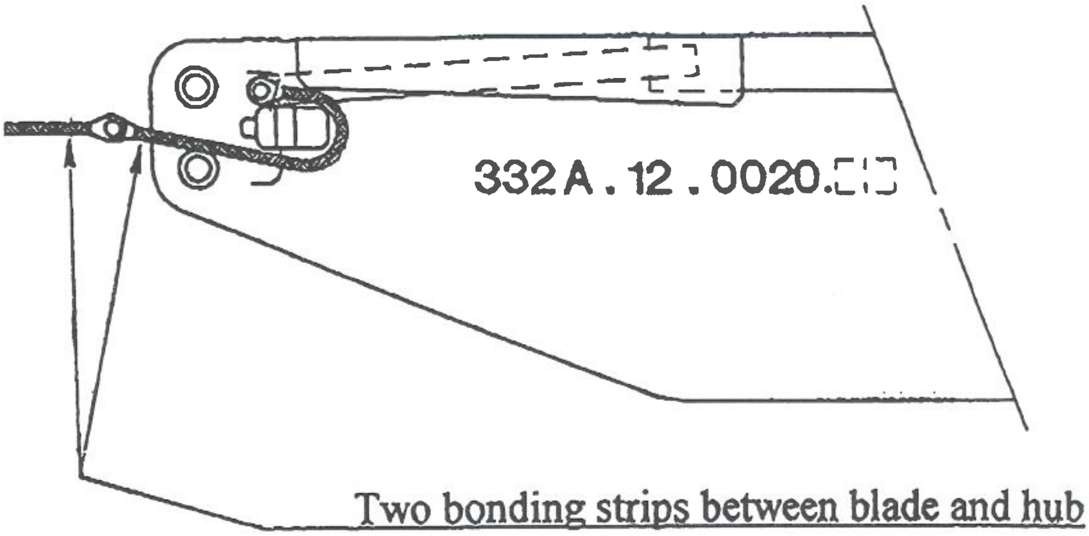

AFTER

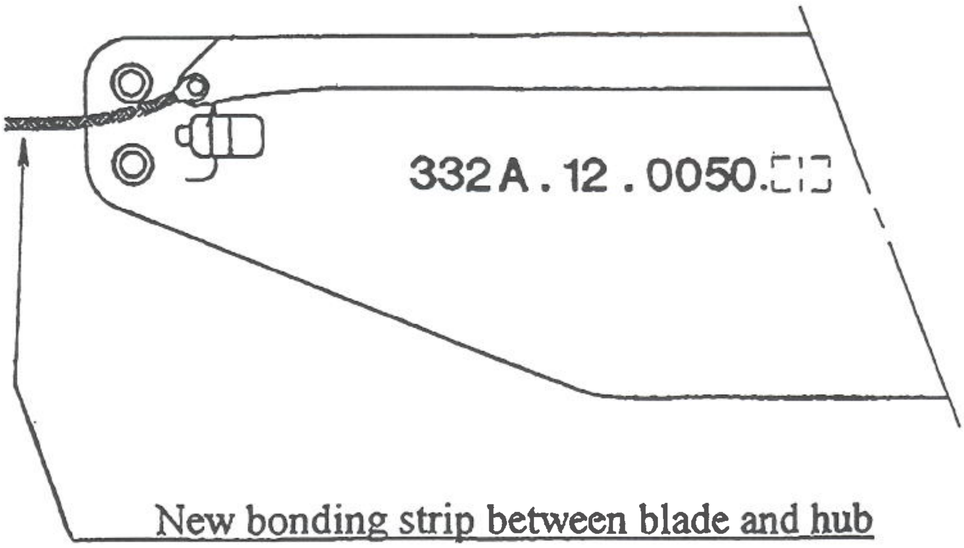

Figure 13C: Showing modified inboard conduction design with replacement of brass strip, which linked erosion shield to root bolt, by extended titanium shield, and fitment of single bonding strap.

APPENDIX D

(FIGURE 1)

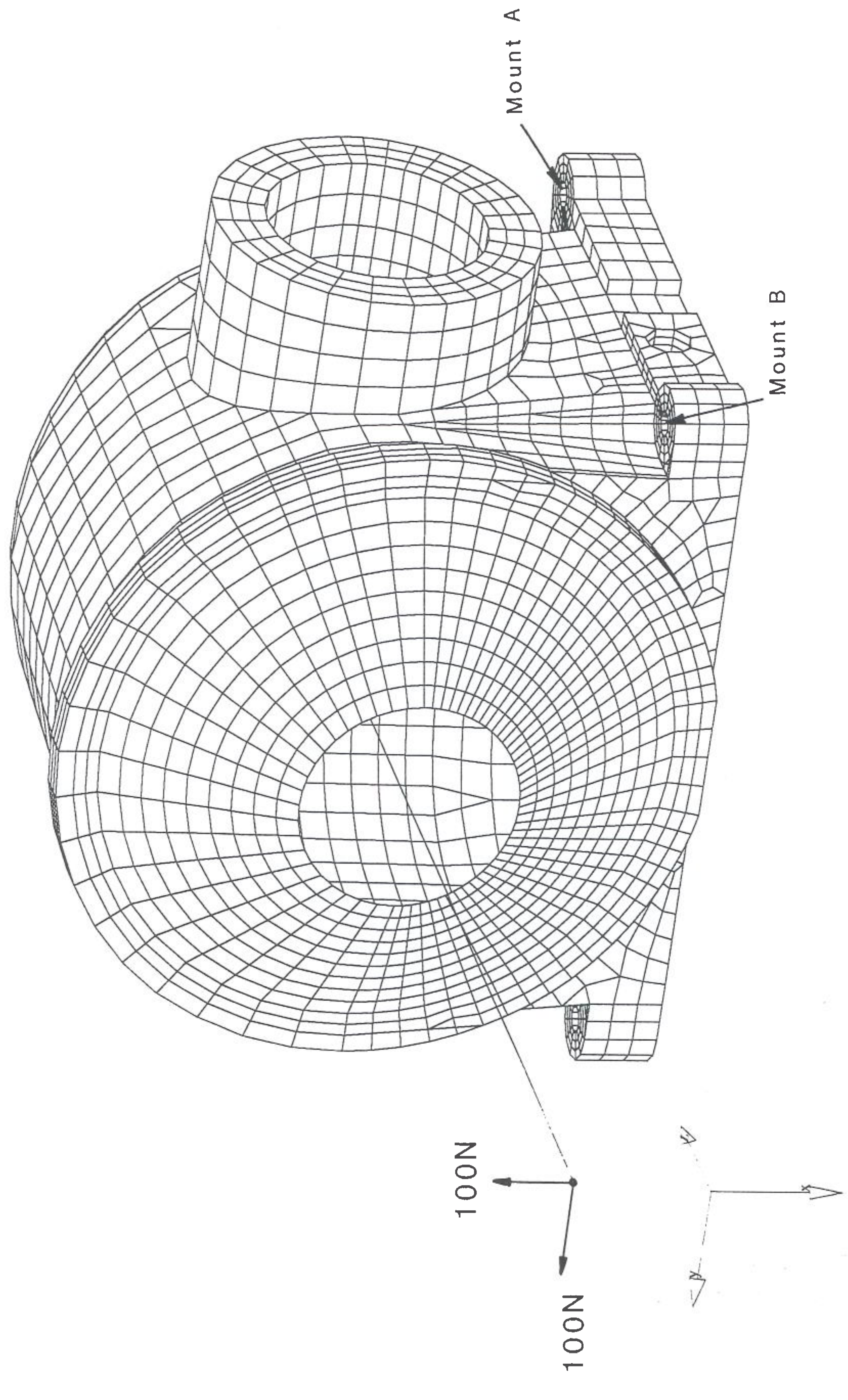

FINITE ELEMENT MODEL SHOWING LOADING LOCATIONS

(FIGURE 2)

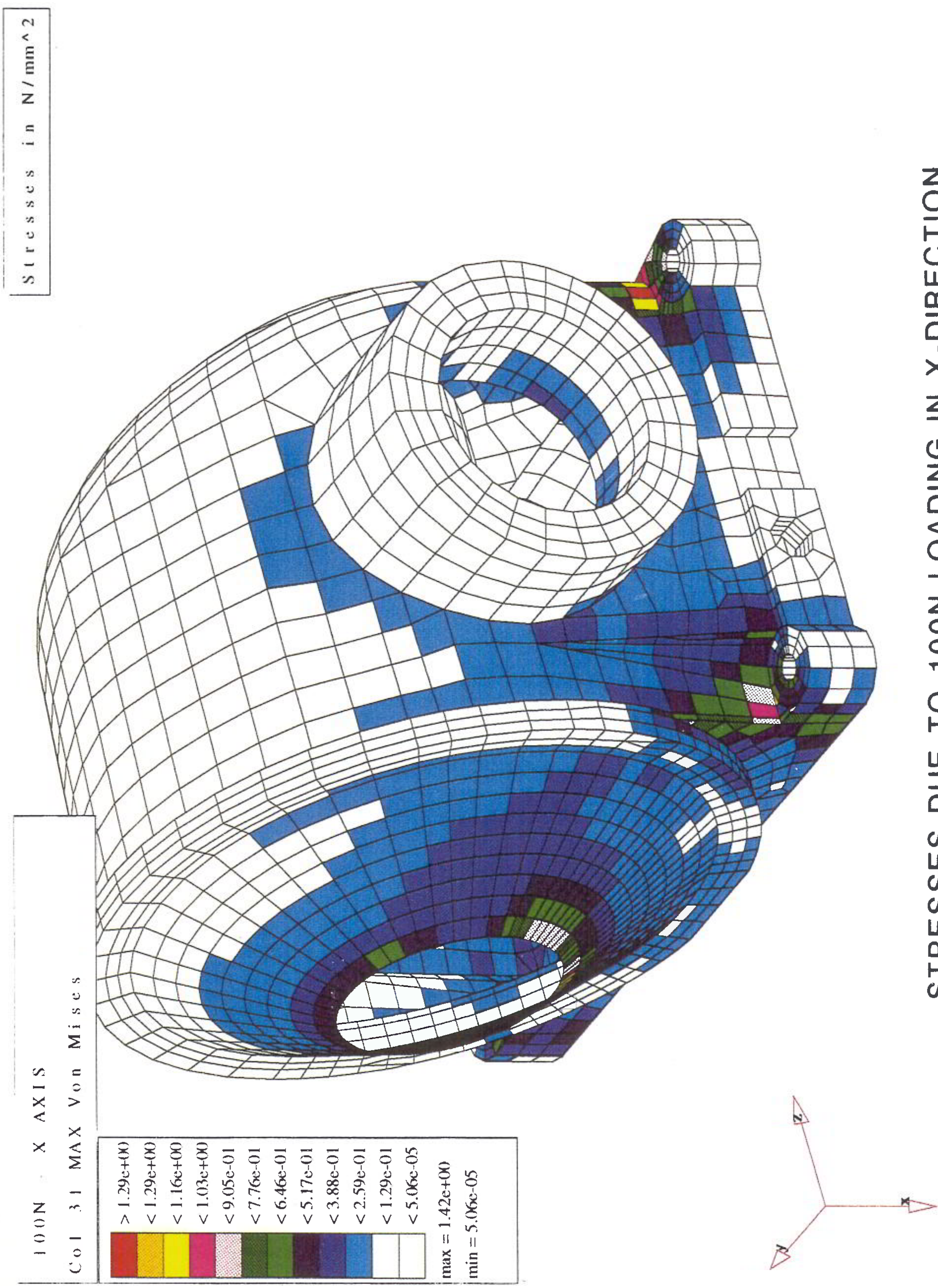

STRESSES DUE TO 100N LOADING IN X-DIRECTION

(FIGURE 3)

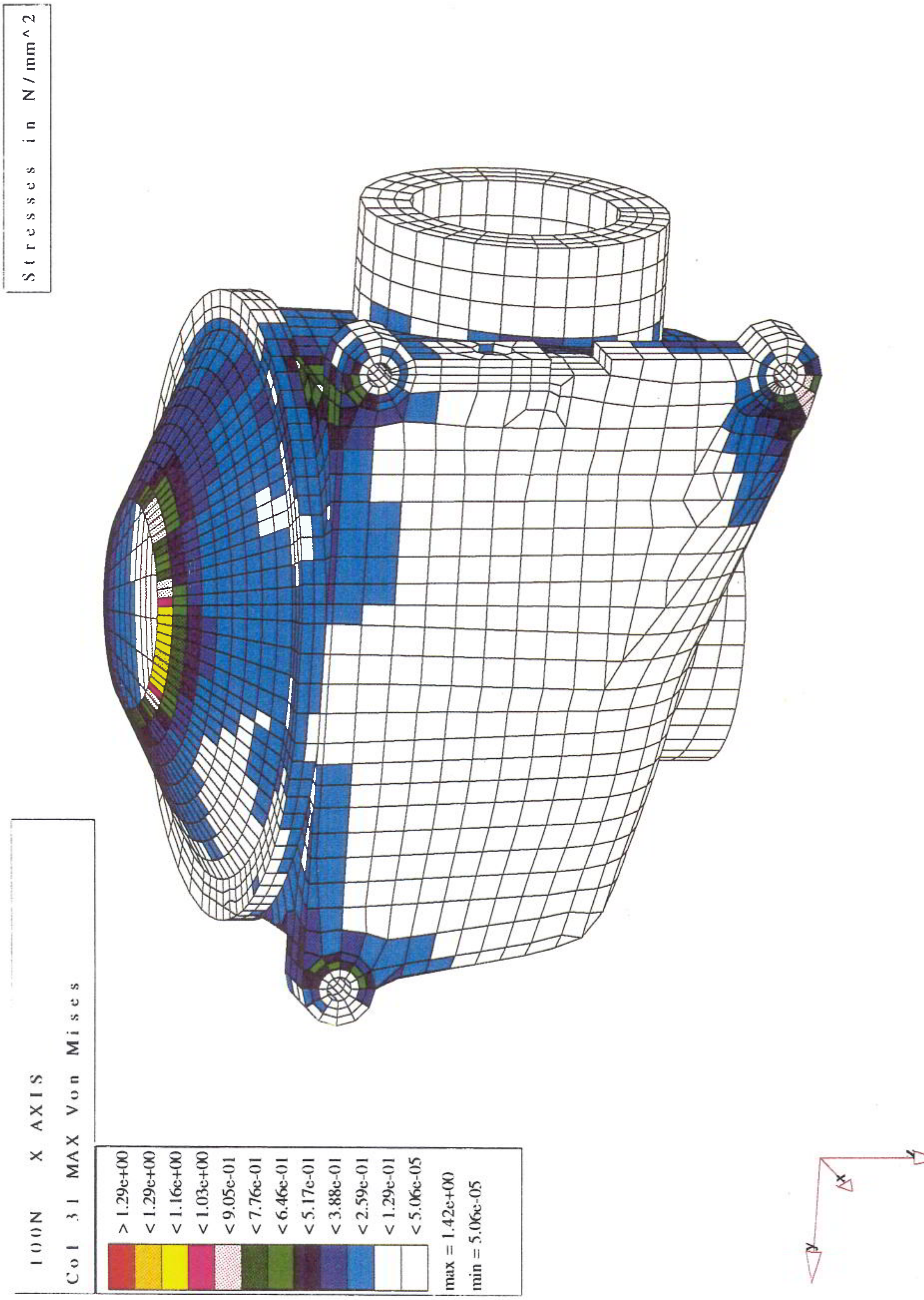

STRESSES DUE TO 100N LOADING IN X-DIRECTION

(FIGURE 4)

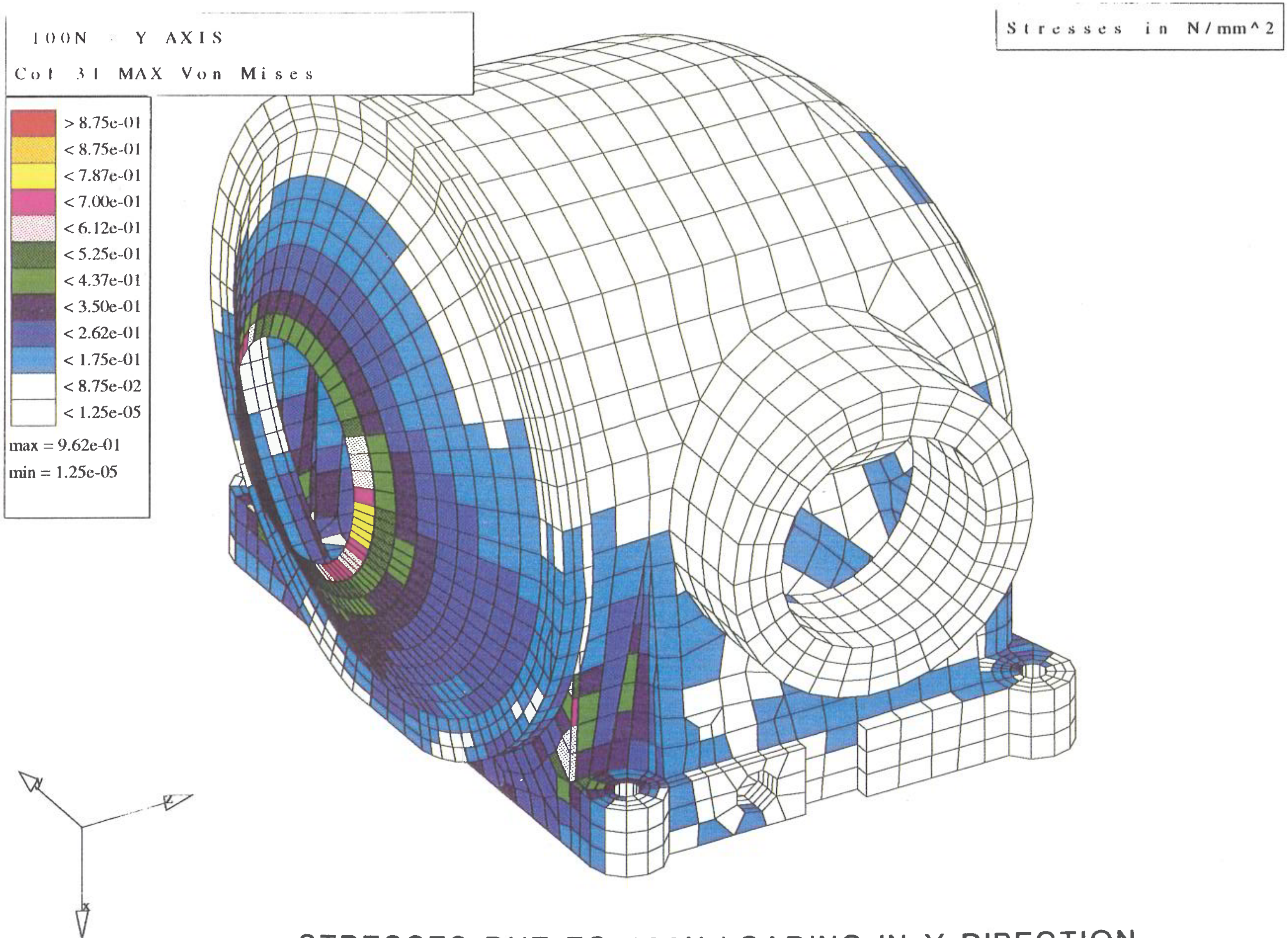

STRESSES DUE TO 100N LOADING IN Y-DIRECTION

(FIGURE 5)

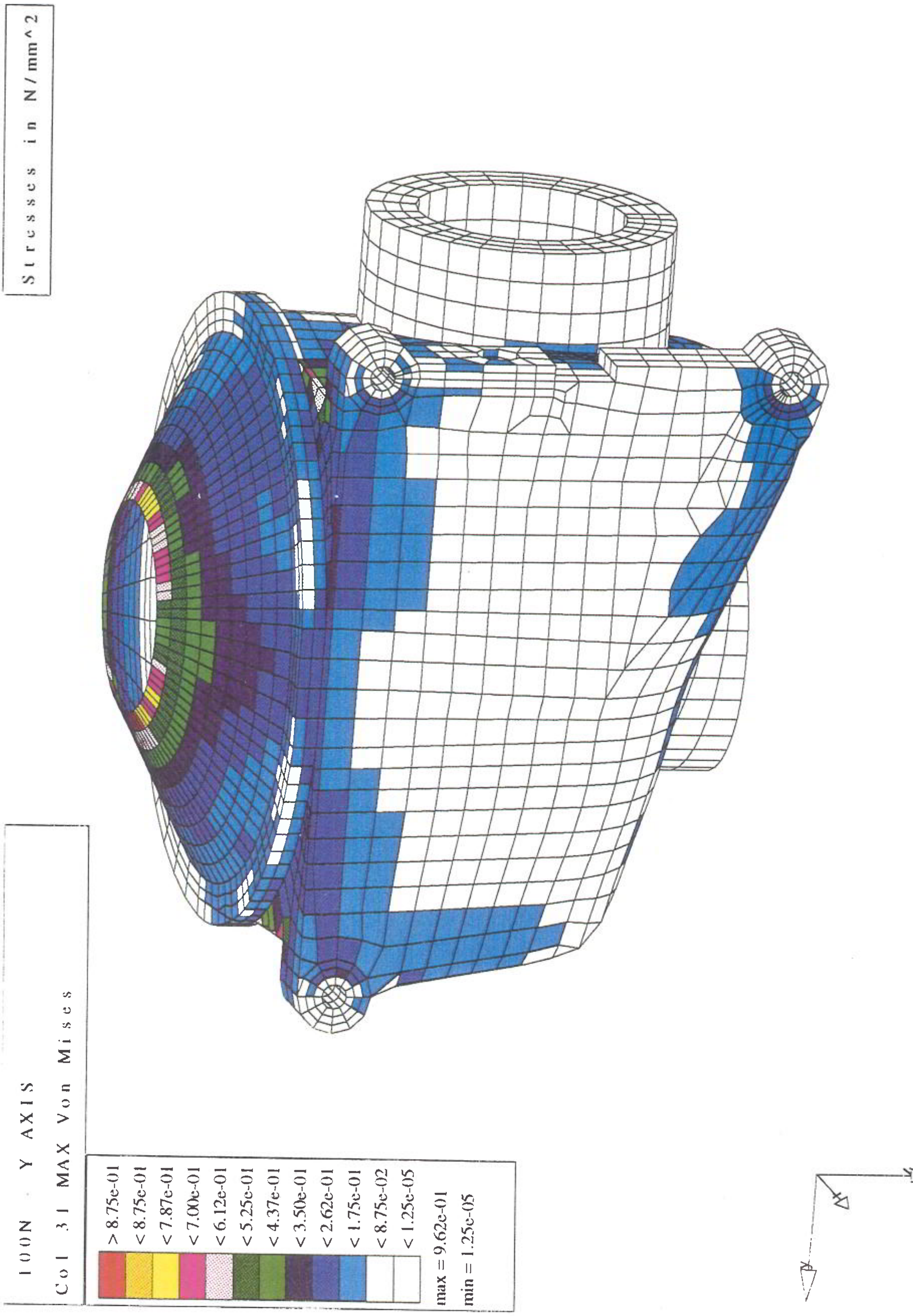

STRESSES DUE TO 100N LOADING IN Y-DIRECTION

APPENDIX E

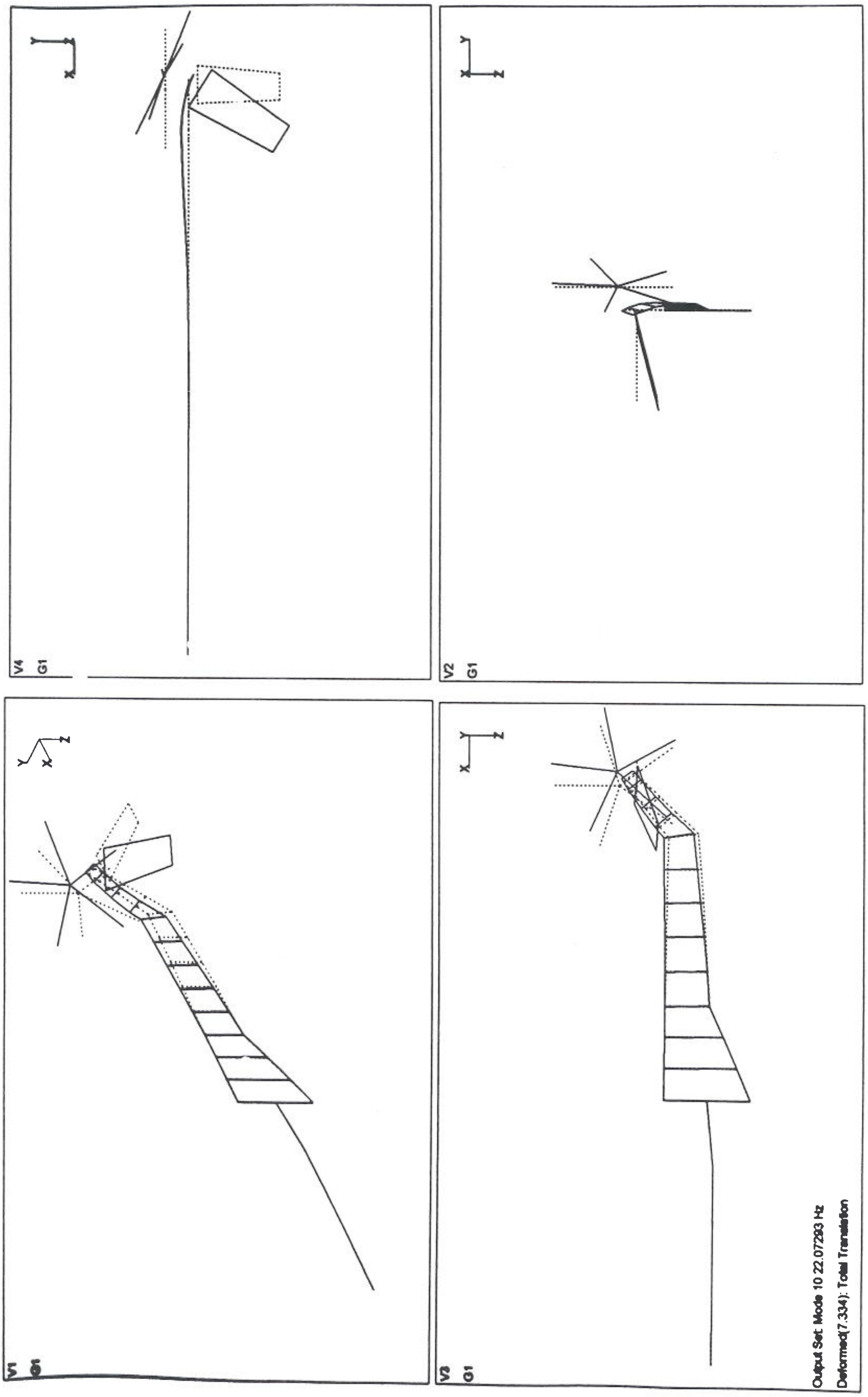

Figure 1: Showing predicted overtone vertical/lateral bending mode at 22.07Hz

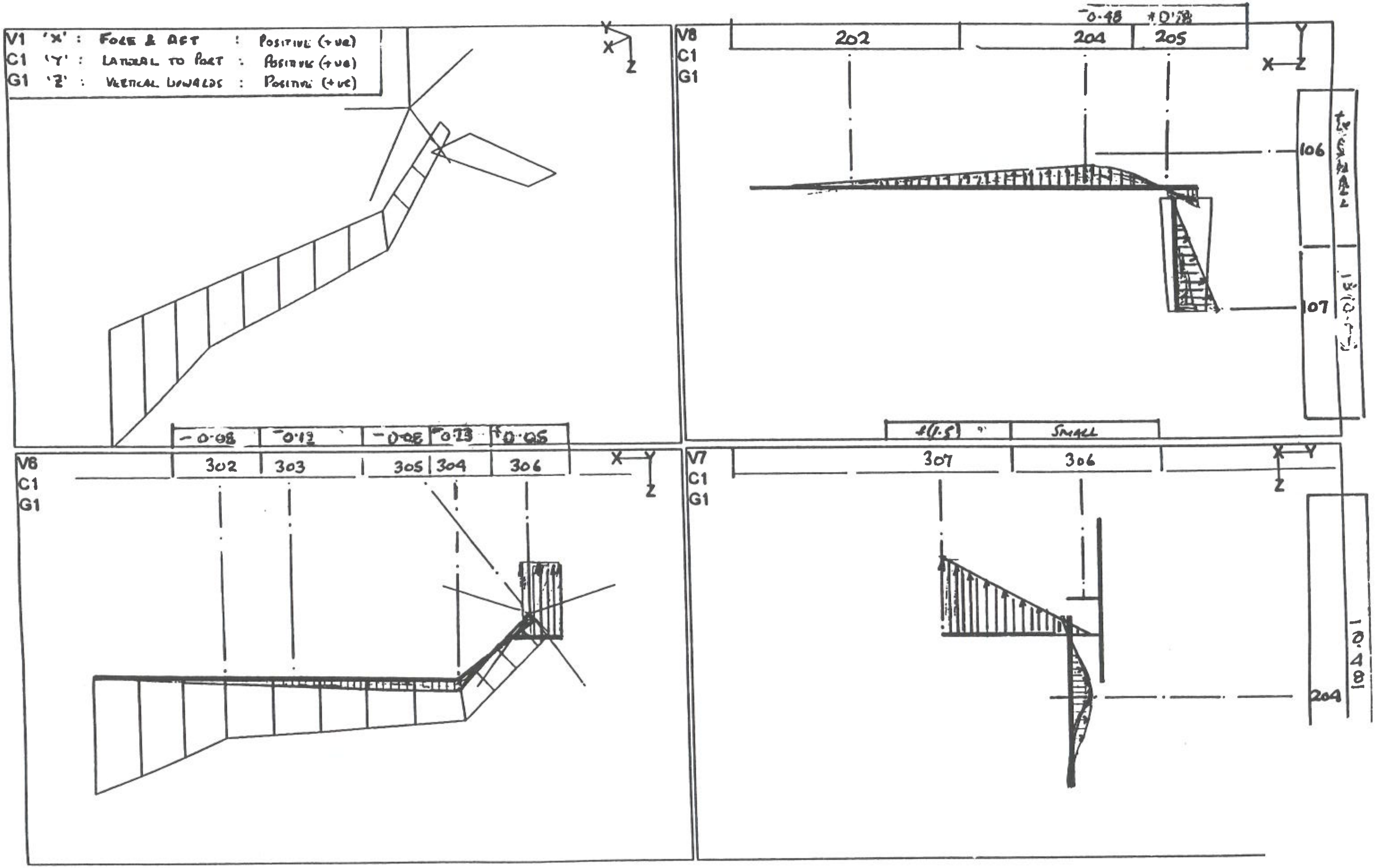

Figure 2: Showing measured overtone vertical/lateral bending and tail roll mode at 22.80Hz

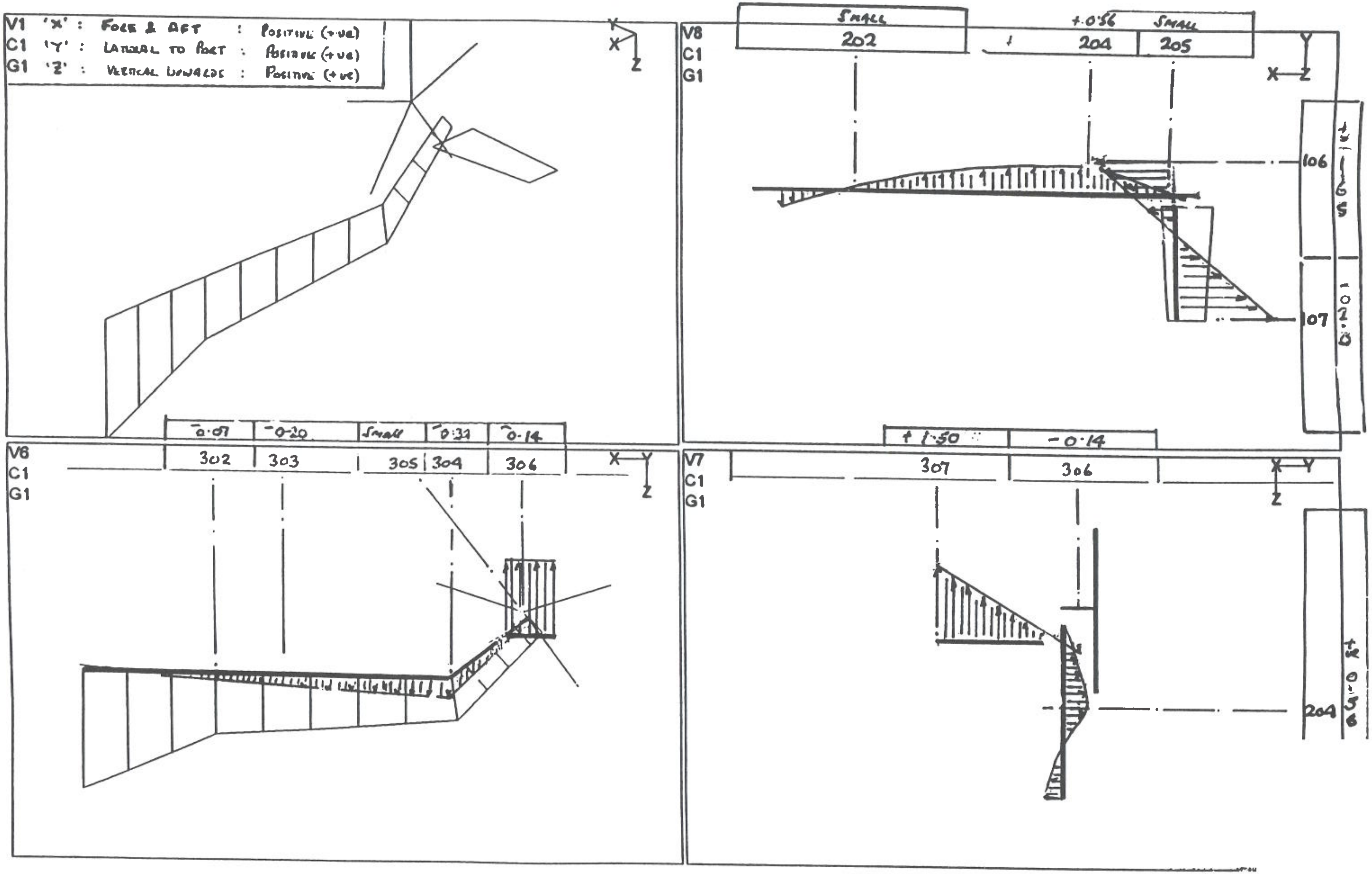

Figure 3: Showing measured overtone vertical/lateral bending with torsion/tailplane yaw mode at 20.80Hz

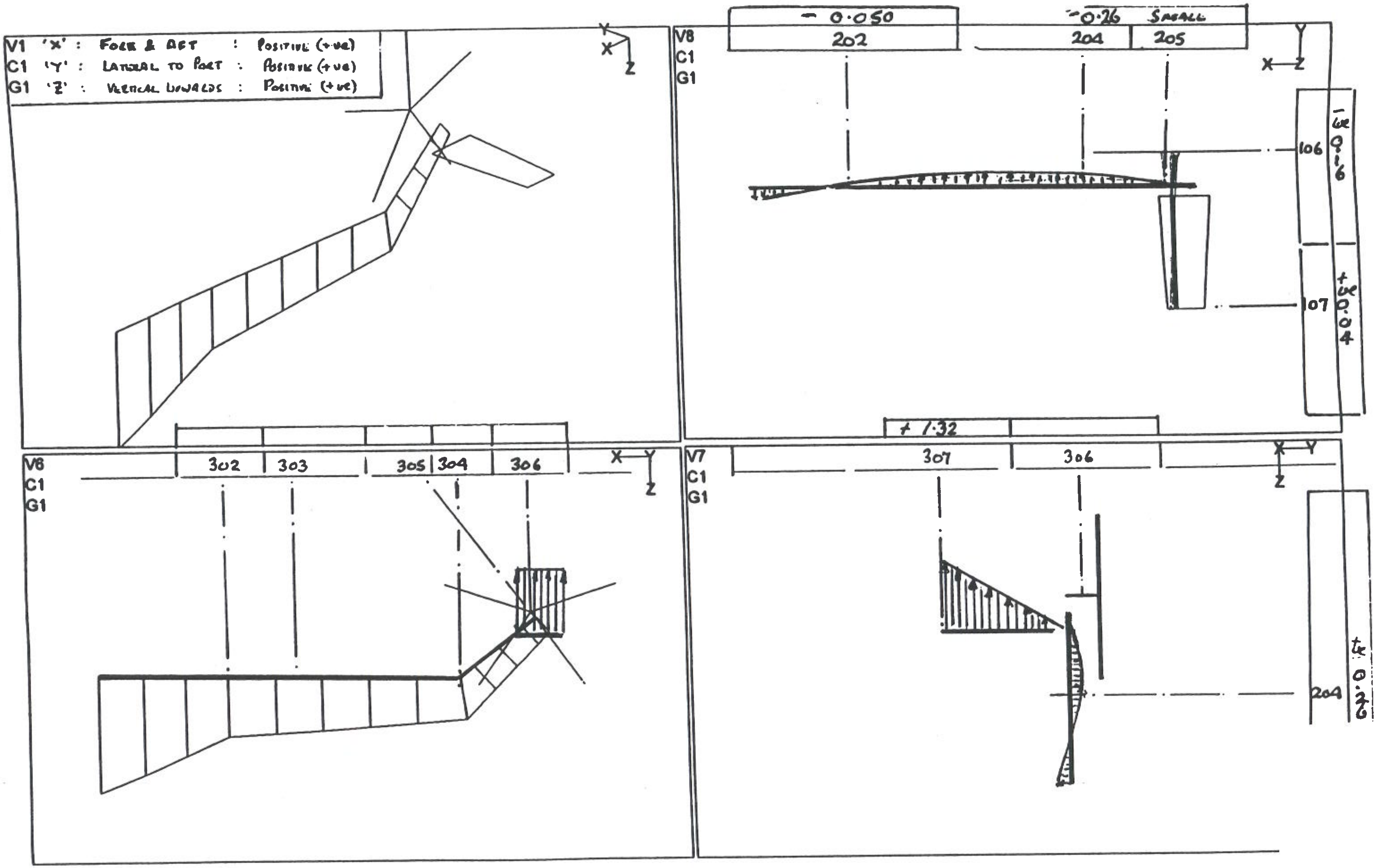

Figure 4: Showing measured overtone lateral bending/tail roll mode at 22.35Hz

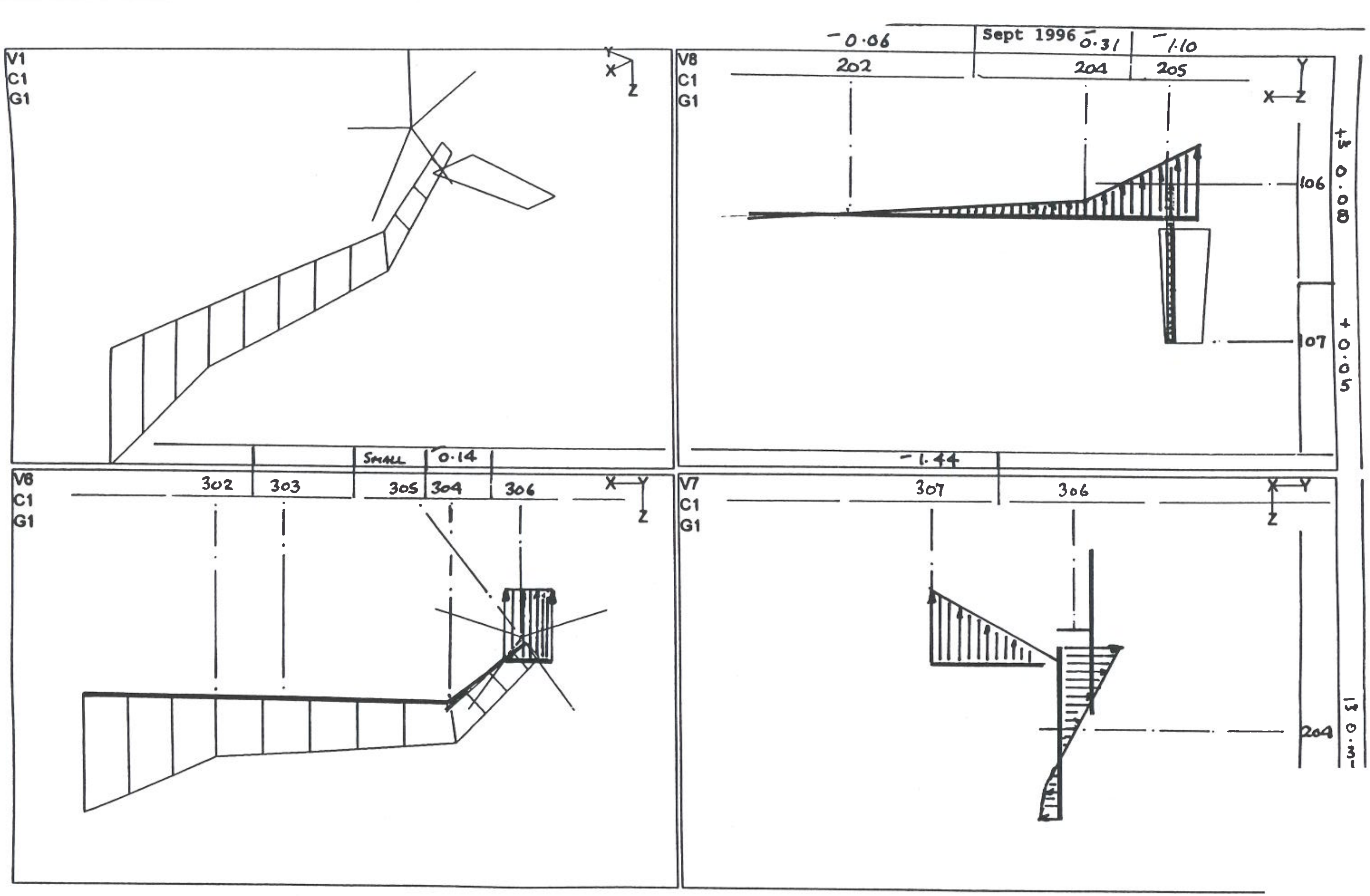

Figure 5: Showing measured lateral bending/tail roll mode at 23.35Hz

MEASURED			PREDICTED	
Mode 7:	20.80 Hz:	Overtone Vert/Lat/ Torsion/Tail Yaw		Aircraft Mode (not represented)
21.56 HZ TAIL ROTOR EXCITATION FREQUENCY IN THIS POSITION				
Mode 8:	22.35 Hz:	Backend Lateral Overtone		Aircraft Mode (not represented)
Mode 9:	**22.80 Hz**	**:Overtone Vert/Lat/Tail Roll**	**Mode 4: 22.07 Hz:**	**Overtone Vert'l/Lateral**
Mode 10:	23.35 Hz	Aircraft Mode Backend		Aircraft Mode (not represented)

Table 1: Showing summary of measured and predicted tail boom/pylon responses

	RIGHT LUG X-AXIS	RIGHT LUG Y-AXIS	RIGHT LUG Z-AXIS	LEFT LUG Z-AXIS	UPPER LUG Y-AXIS	UPPER LUG Z-AXIS	AVIONICS BAY ACCN.
NEWTONS	36,650	40,000	14,300	17,100	39,700	30,500	6.4G
lbf	8,239	8,992	3,215	3,844	8,925	6,857	

Table 2: Showing calculated dynamic forces on the tail rotor gearbox attachment lugs and G-switch due to out-of-balance effects induced by loss of the anti-erosion shield from one tail rotor blade (X-axis normal to gearbox mounting plane, Y-axis parallel/longitudinal to mounting plane and Z-axis parallel/lateral to mounting plane).

Printed in the United Kingdom for the Stationery Office
C5 9/97 65536 N34673 32/39564